ARICH experience in Belle II

Samo Korpar

University of Maribor and Jožef Stefan Institute, Ljubljana
5 October 2023, ePIC pfRICH General meeting

Outline:

- ARICH at Belle II
- ARICH detector:
  - aerogel radiator
  - HAPD photon detector
  - front-end electronics
- Operation status
- Calibration and Alignment
- PDF, likelihood and PID performance

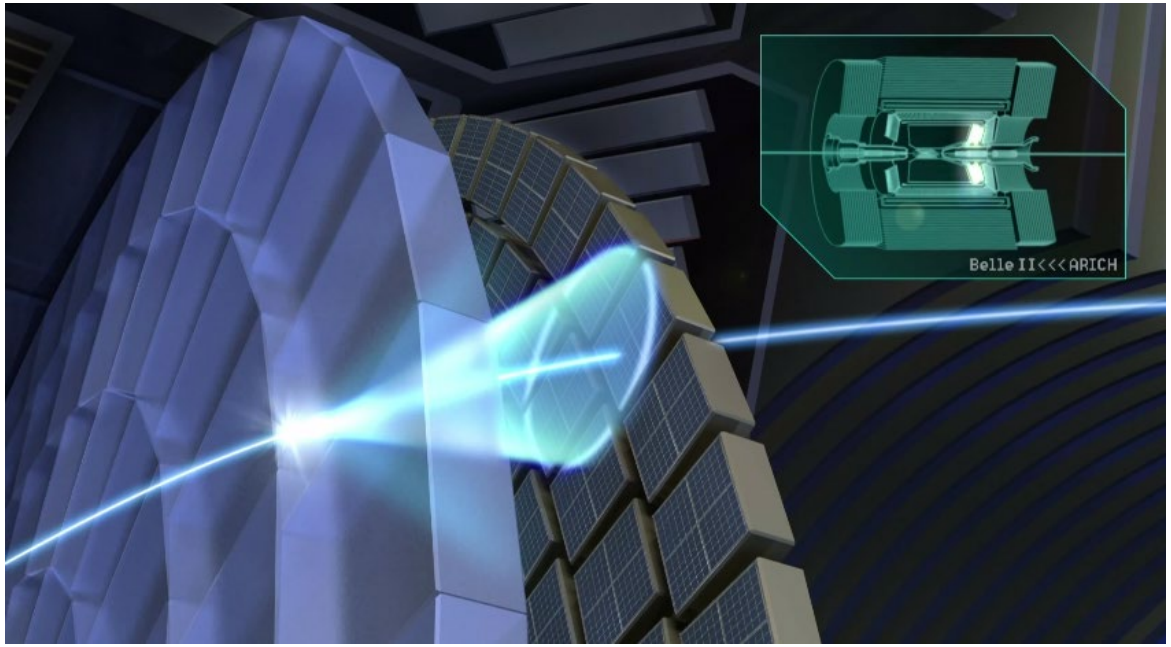

Belle II spectrometer

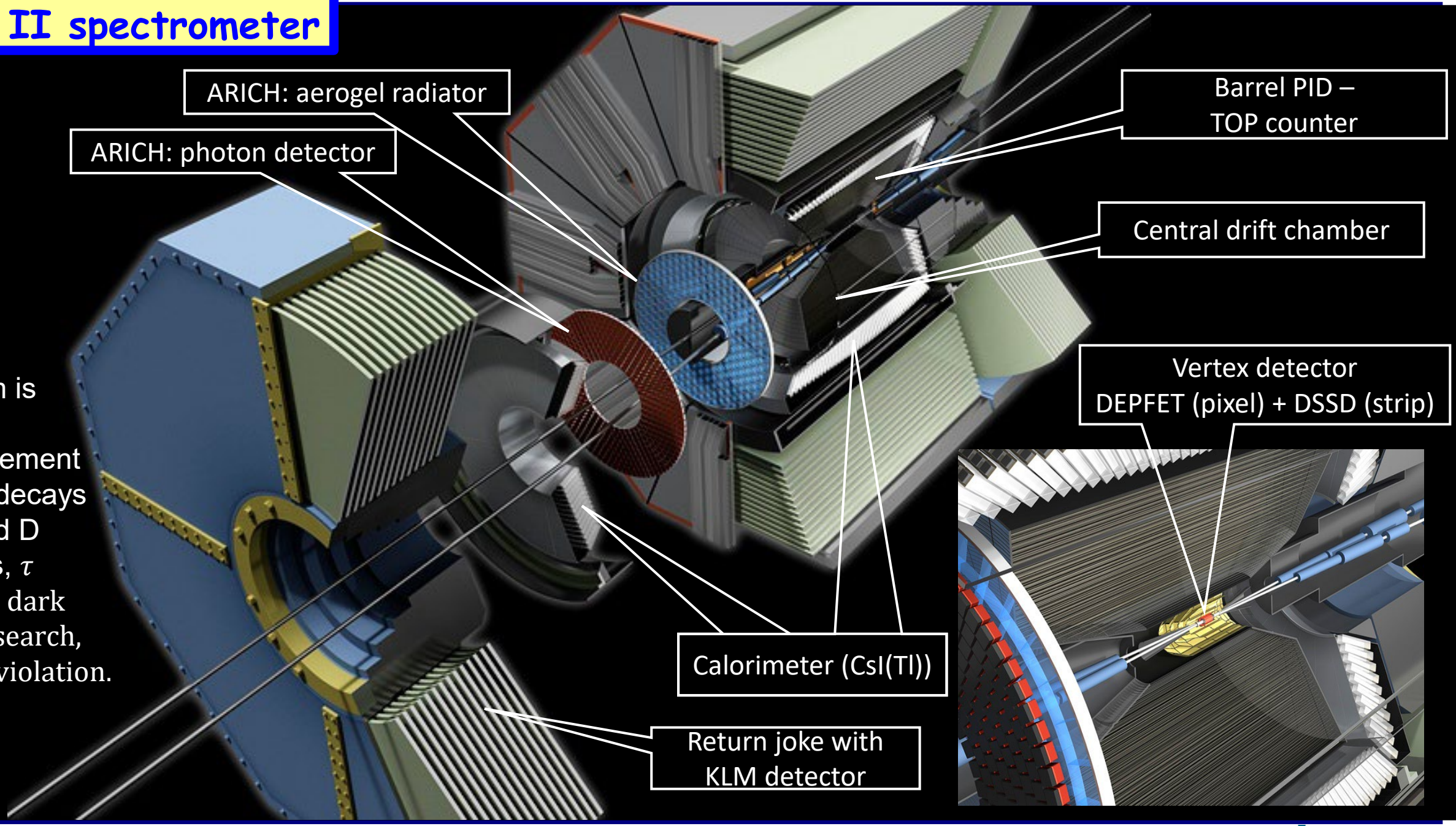

The aim is precise measurement of rare decays of B and D mesons, τ leptons, dark matter search, and CP violation.

ARICH - basics

Proximity focusing Aerogel Ring Imaging CHerenkov detector (ARICH) components:

- double layer focusing aerogel radiator (20 mm + 20 mm)
- 160 mm expansion gap
- photon detector based on 420 Hybrid Avalanche Photo Detectors (HAPD)
- front-end electronics with dedicated ASICs, and FPGAs

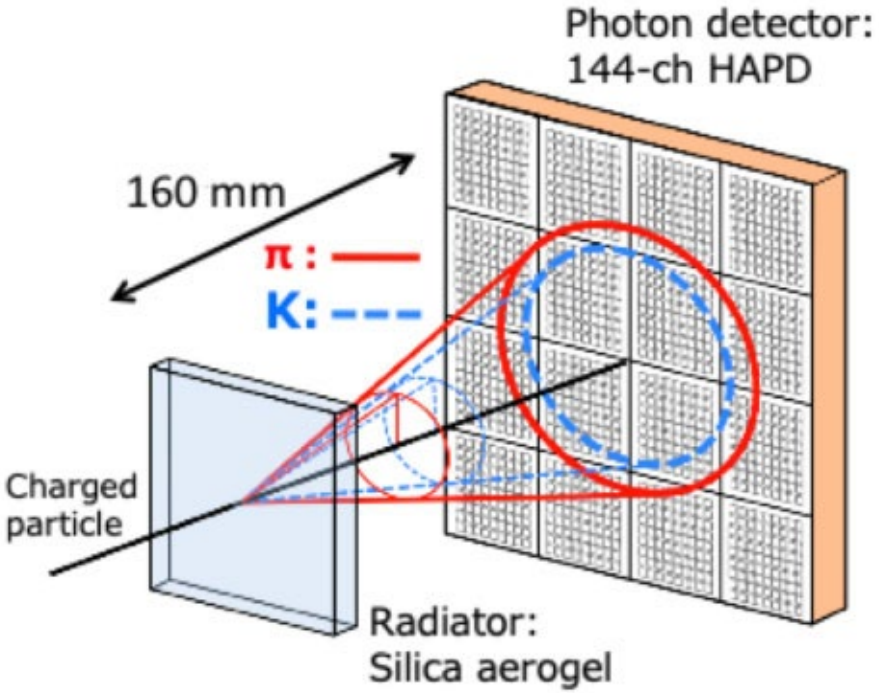

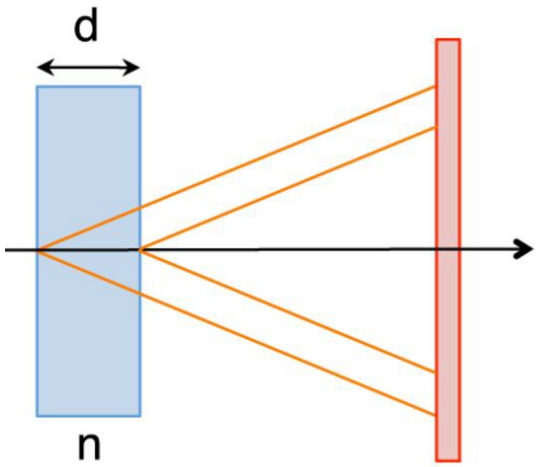

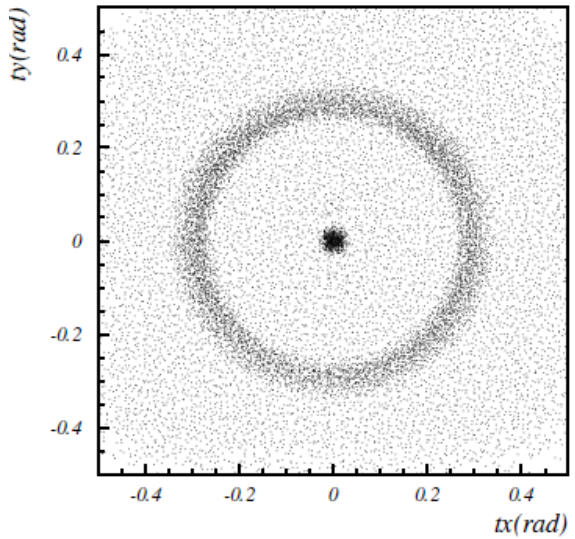

Single-layer system

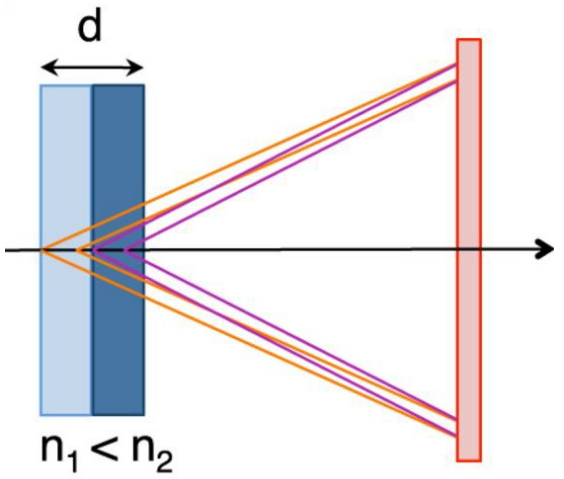

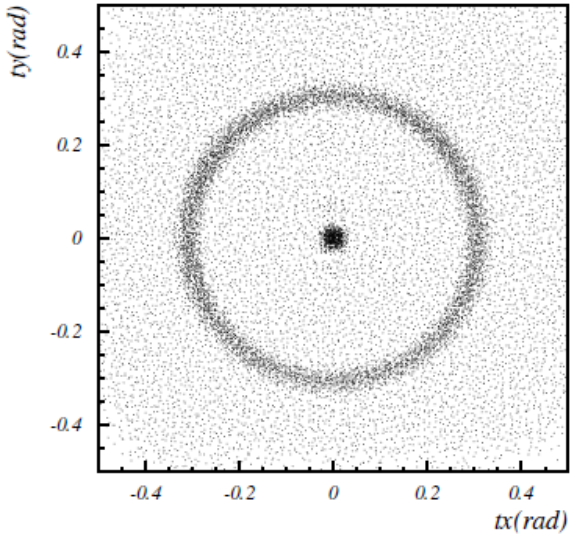

Dual-layer system

Aerogel improvement during ARICH R&D

- improved transparency of conventional aerogels
- used for final production

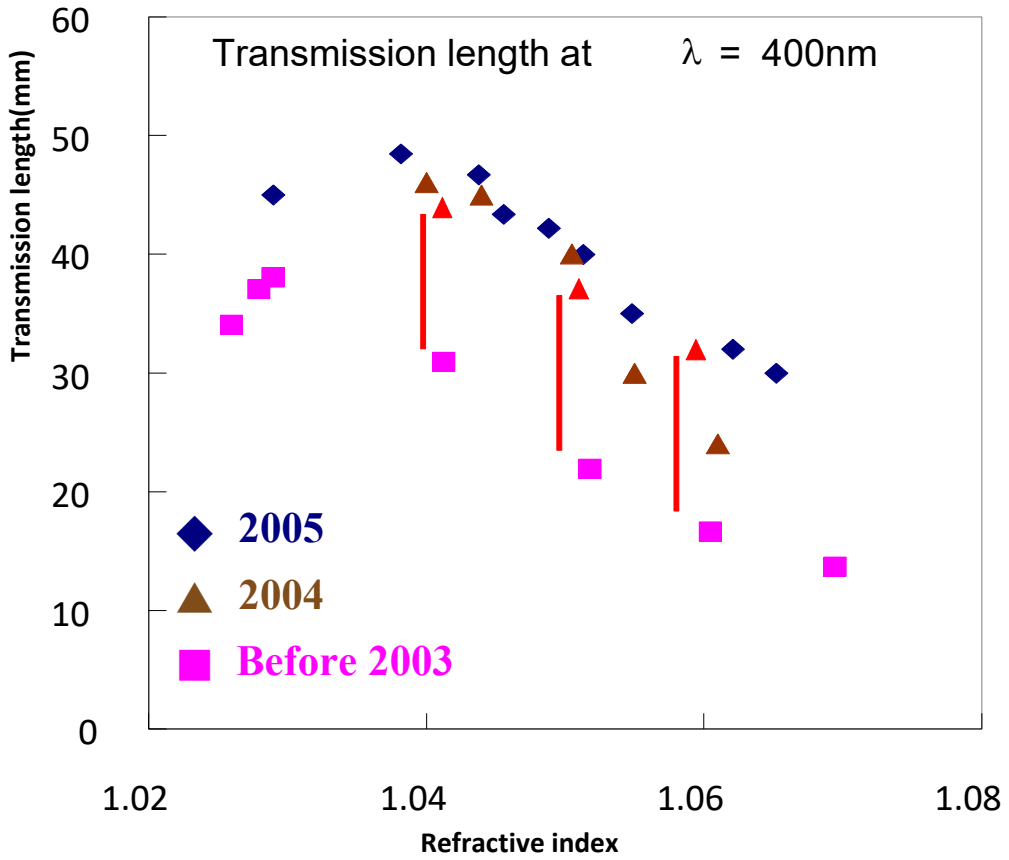

- transparency further improved with pinhole drying method
- problems with production of large tiles (frequent cracks)

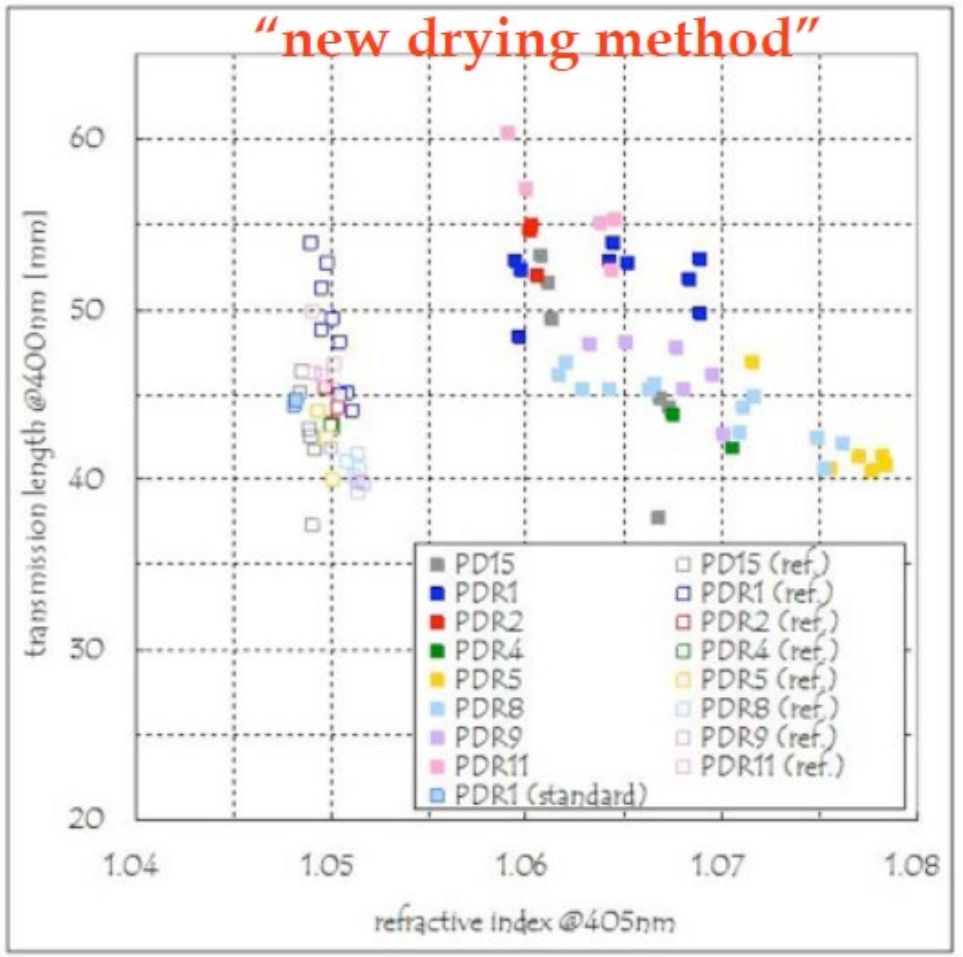

M. Tabata et. al. @ TIPP 2011

Aerogel radiator

- two layers of 20 mm thick hydrophobic aerogel:
  - upstream, n $\approx 1.045, \lambda_{400\,nm} \approx 45$ mm
  - downstream, $n = 1.055$, $\lambda_{400nm} \approx 35$ mm
- 4 segmented rings, 2×124 tiles
- all but exit surface of each pair covered by black paper
- each pair fixed by two black strings running radially
- completed in December 2016

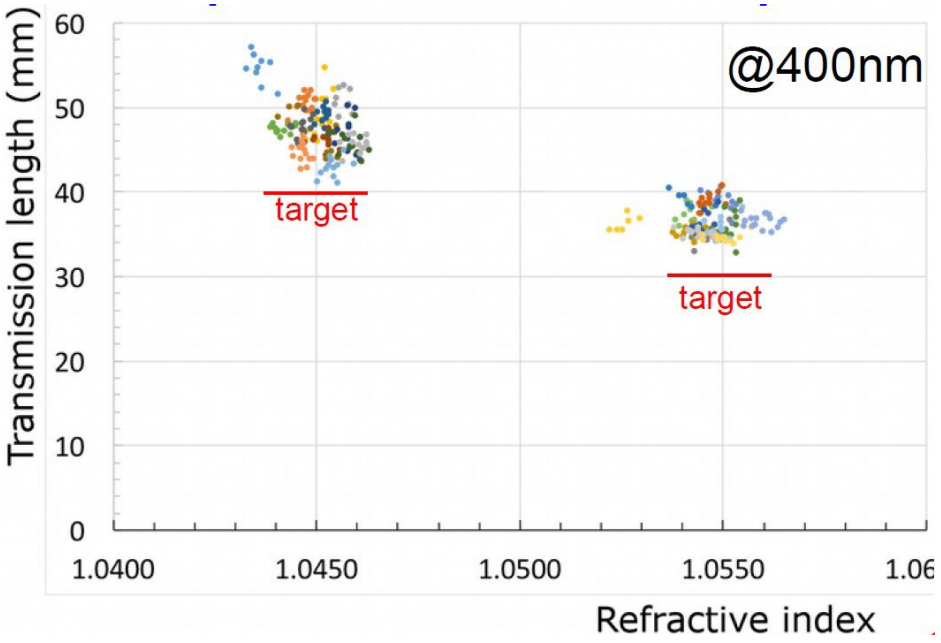

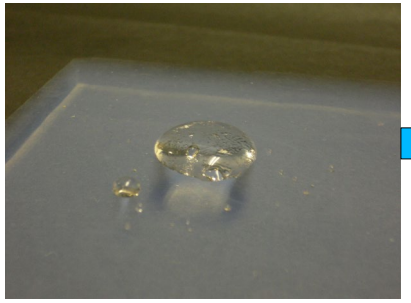

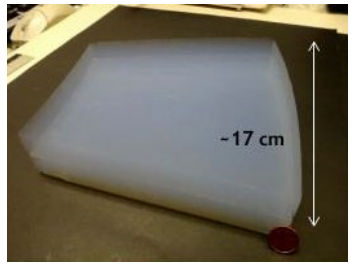

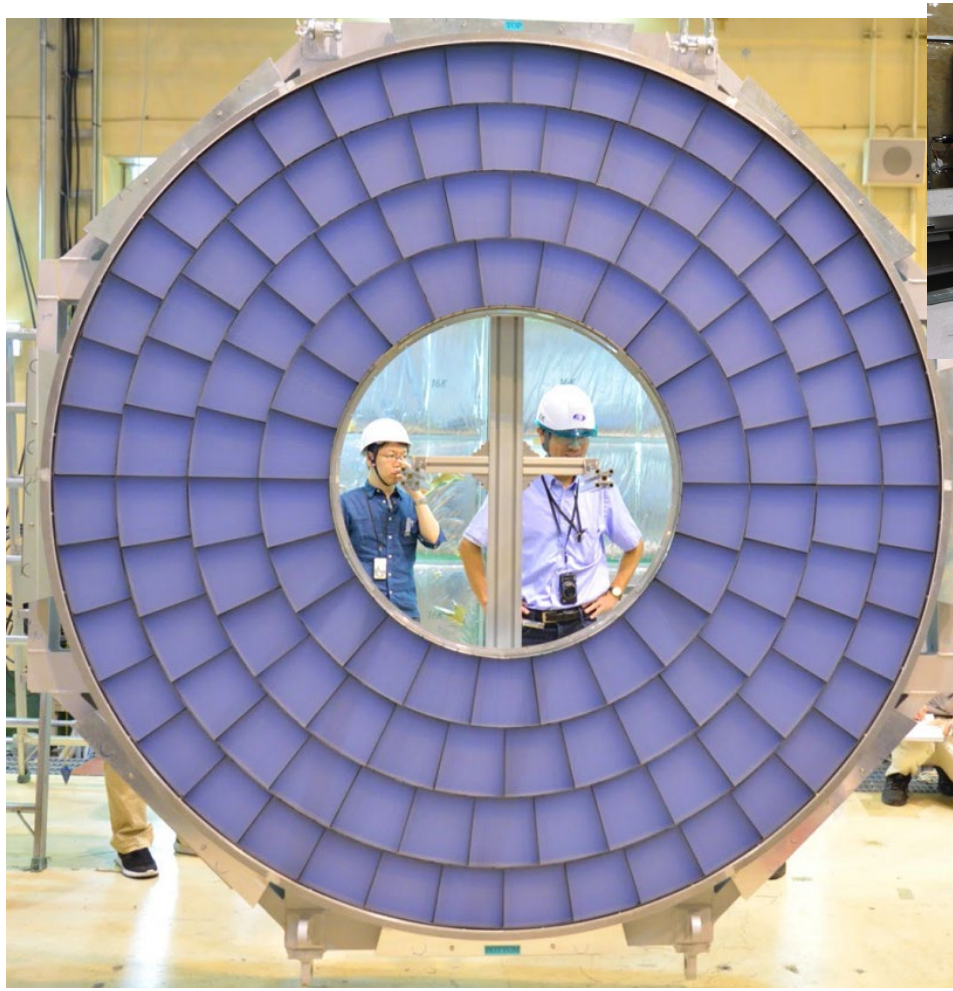

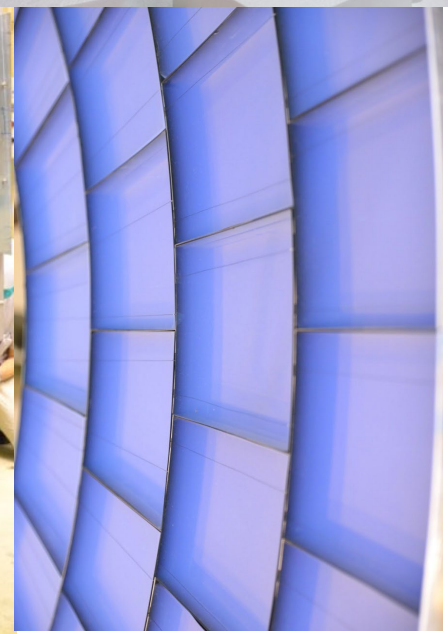

Photon detector - HAPD

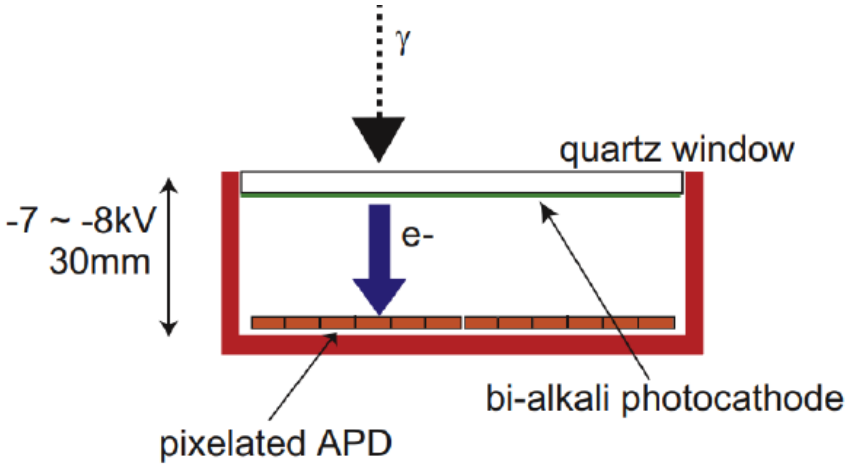

Photon detector is constructed from 420 HAPD modules.

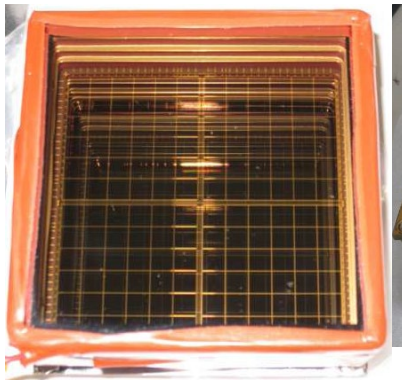

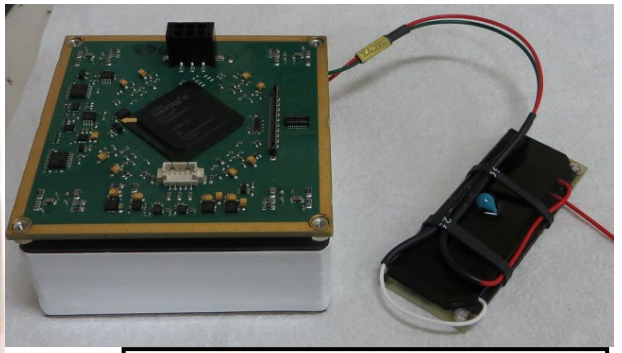

HAPD properties:

- size: $73 \times 73 \times 28\ \mathrm{mm}^3$
- 2×2 APDS with 6×6 channels, $4.9 \times 4.9\ \mathrm{mm}^2$ @ 5.1mm pitch
- $< QE_{400nm} > \approx 32\ \%$
- combined gain $\approx 70\mathrm{k}$
- channel capacitance $80\ \mathrm{pF}$
- operation in $\mathrm{B} = 1.5\ \mathrm{T}$
- radiation tolerance $\approx 10^{12}\ \frac{n_{1MeV}}{\mathrm{cm}^2}$

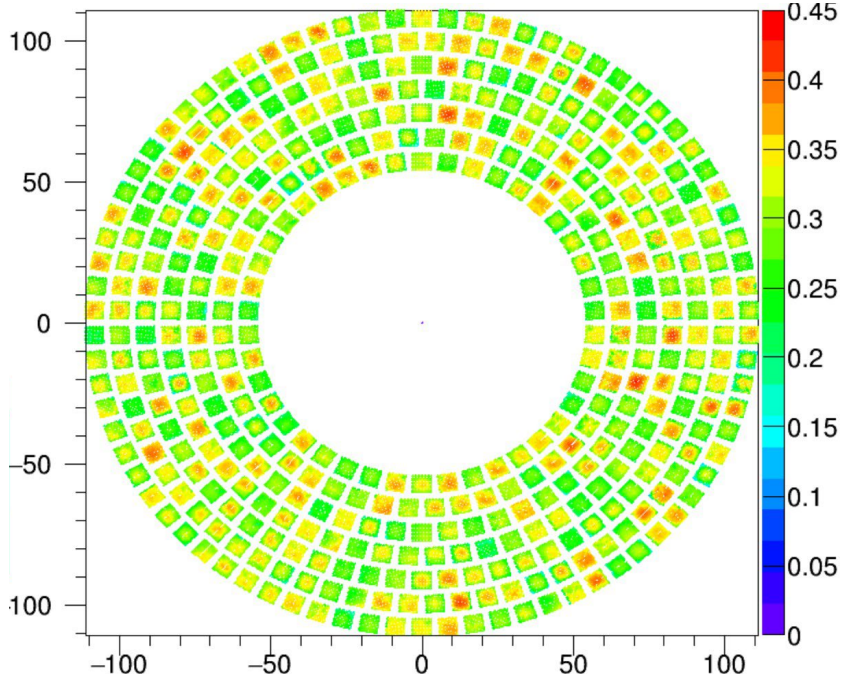

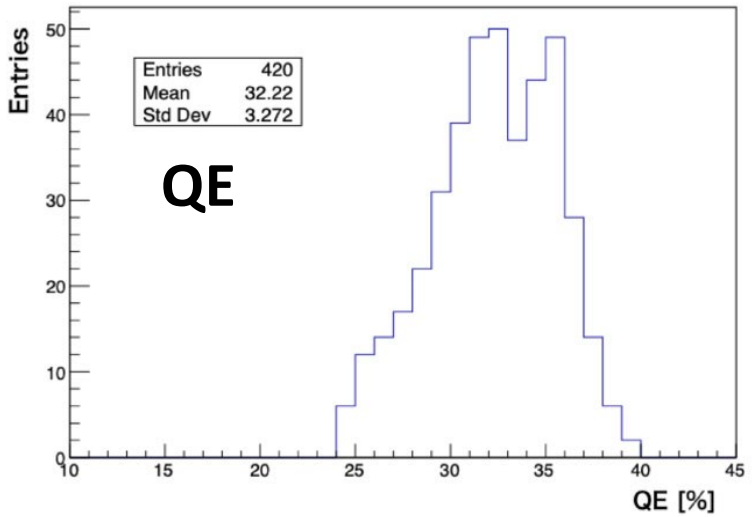

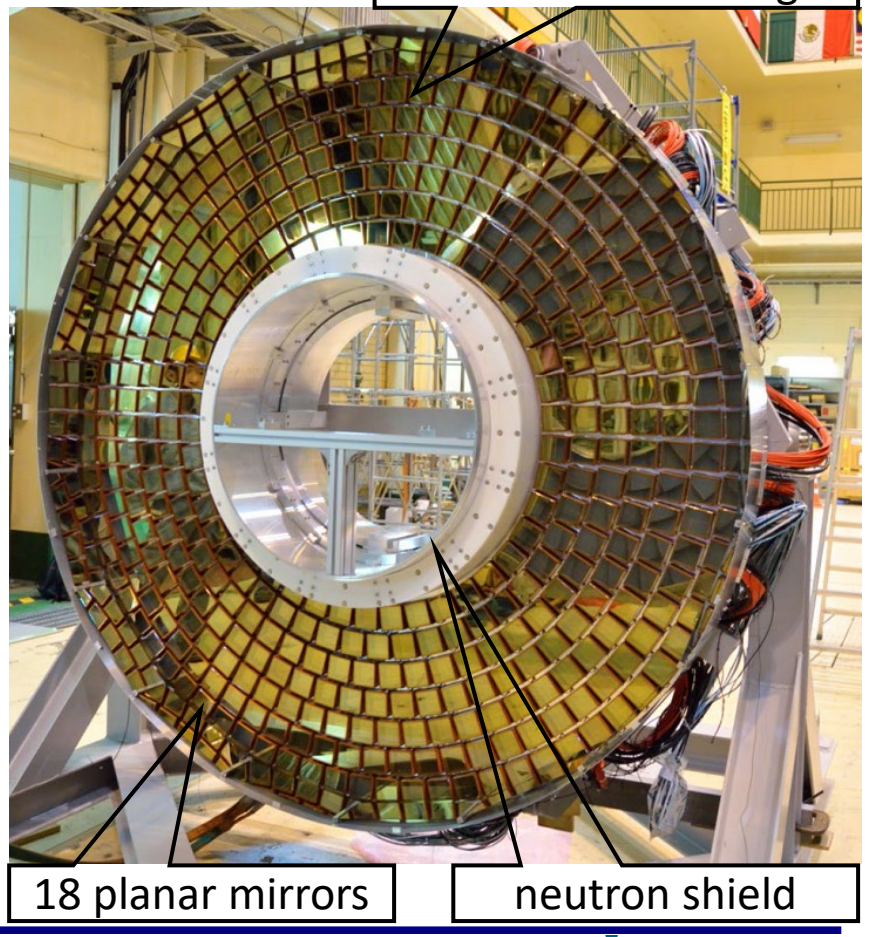

Front-end electronics

Front-end electronics is organized in units of one merger board (MB) controling 6 (or 5) front-end boards (FEB)

- FEB is based on 4 36 ch. ASICs each covering one APD, and Spartan-6 FPGA
- MB controls FEB slow control parameters, and collects and transfers data to back-end DAQ

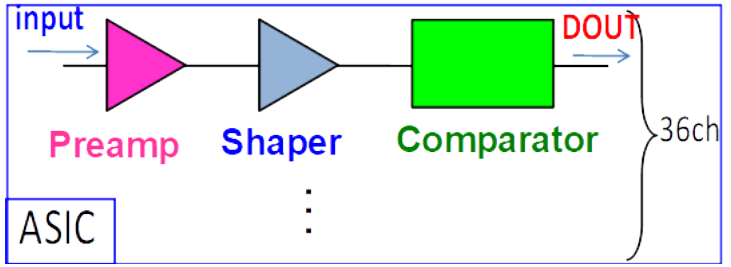

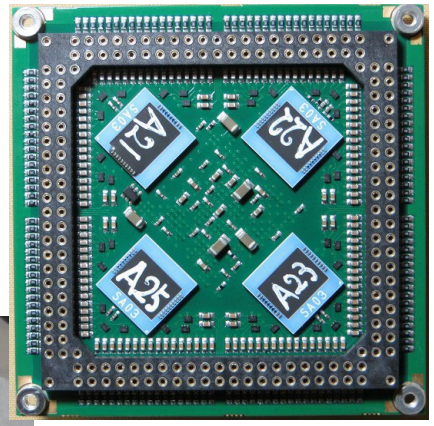

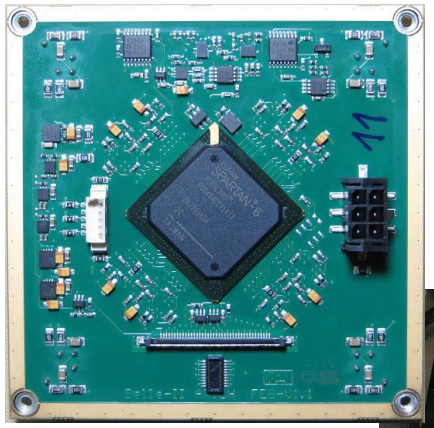

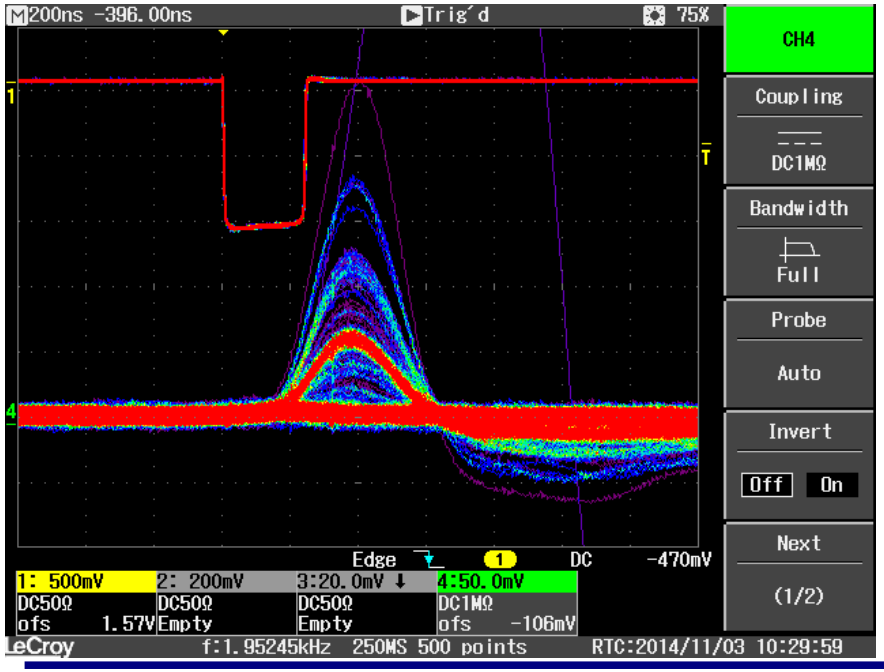

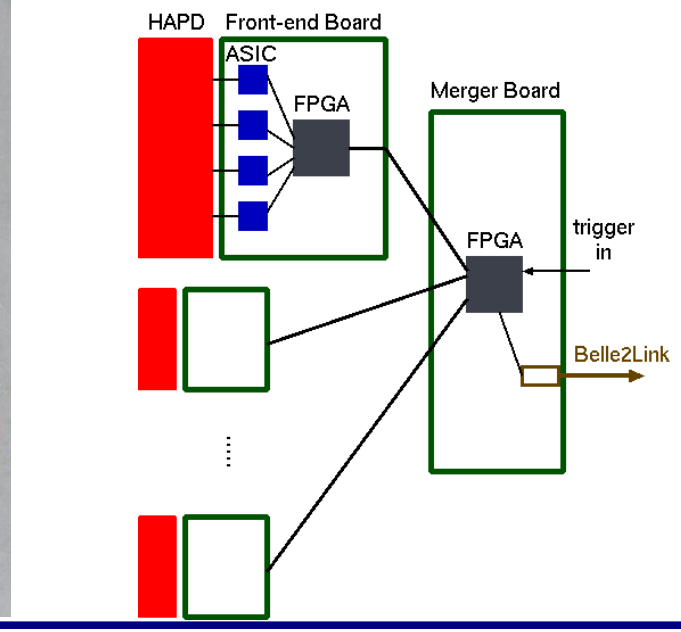

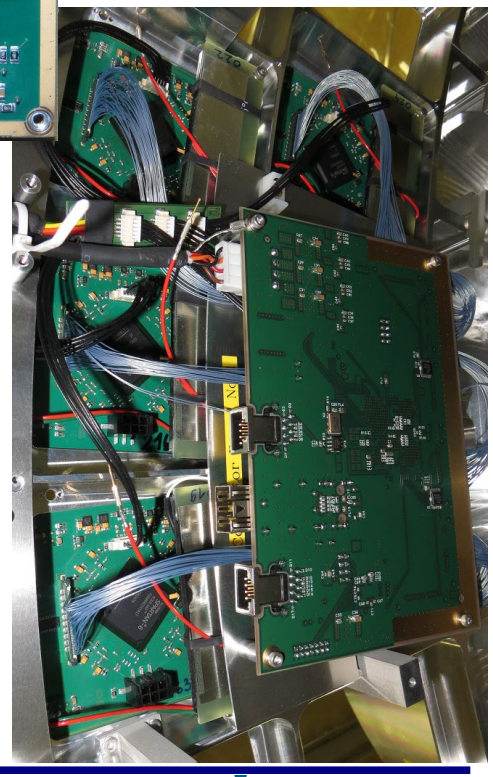

ARICH integration

Joining radiator and photon detector parts in 2017.

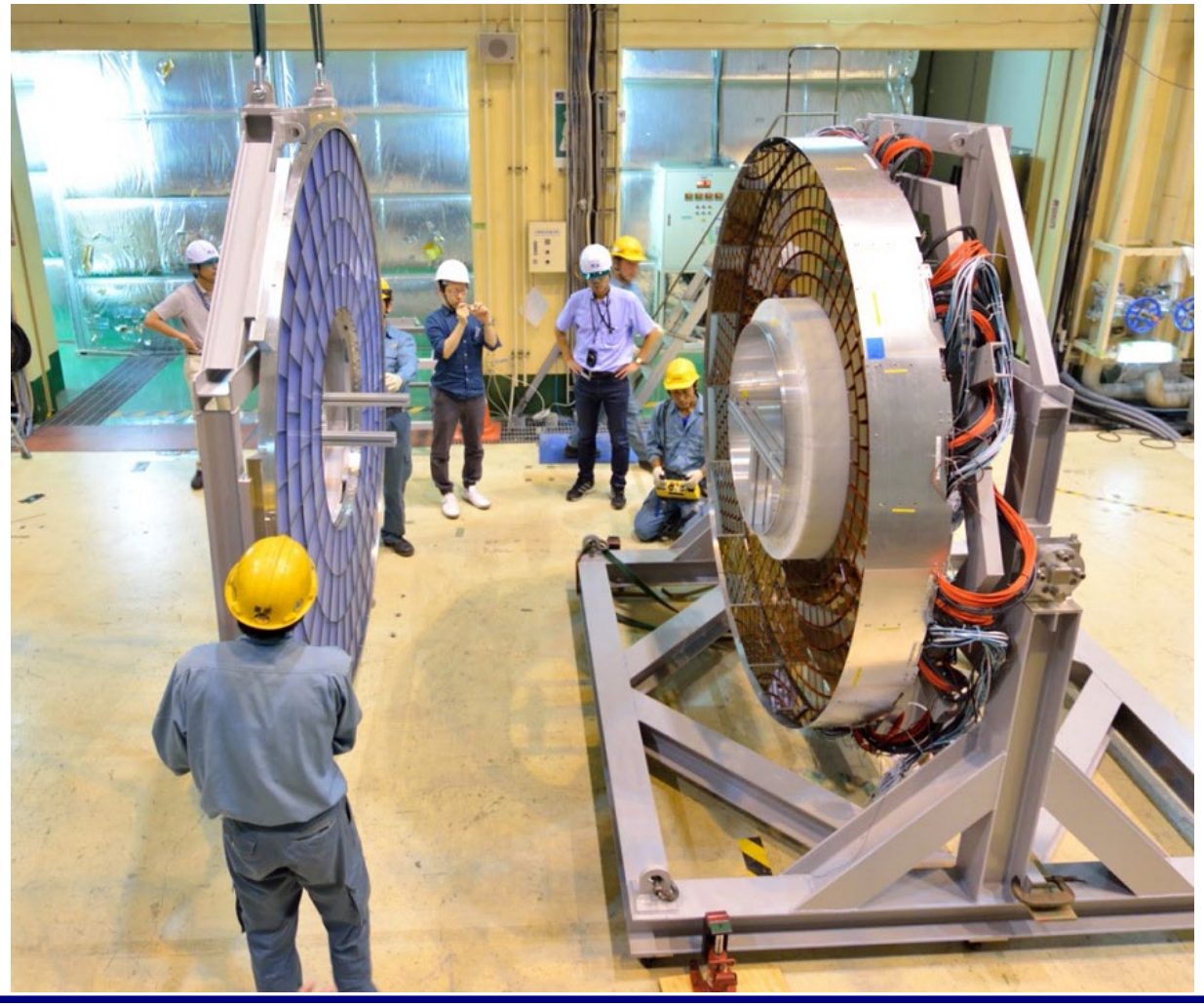

Back side view of ARICH with FE boards, cooling system, cabling and merger boards on top.

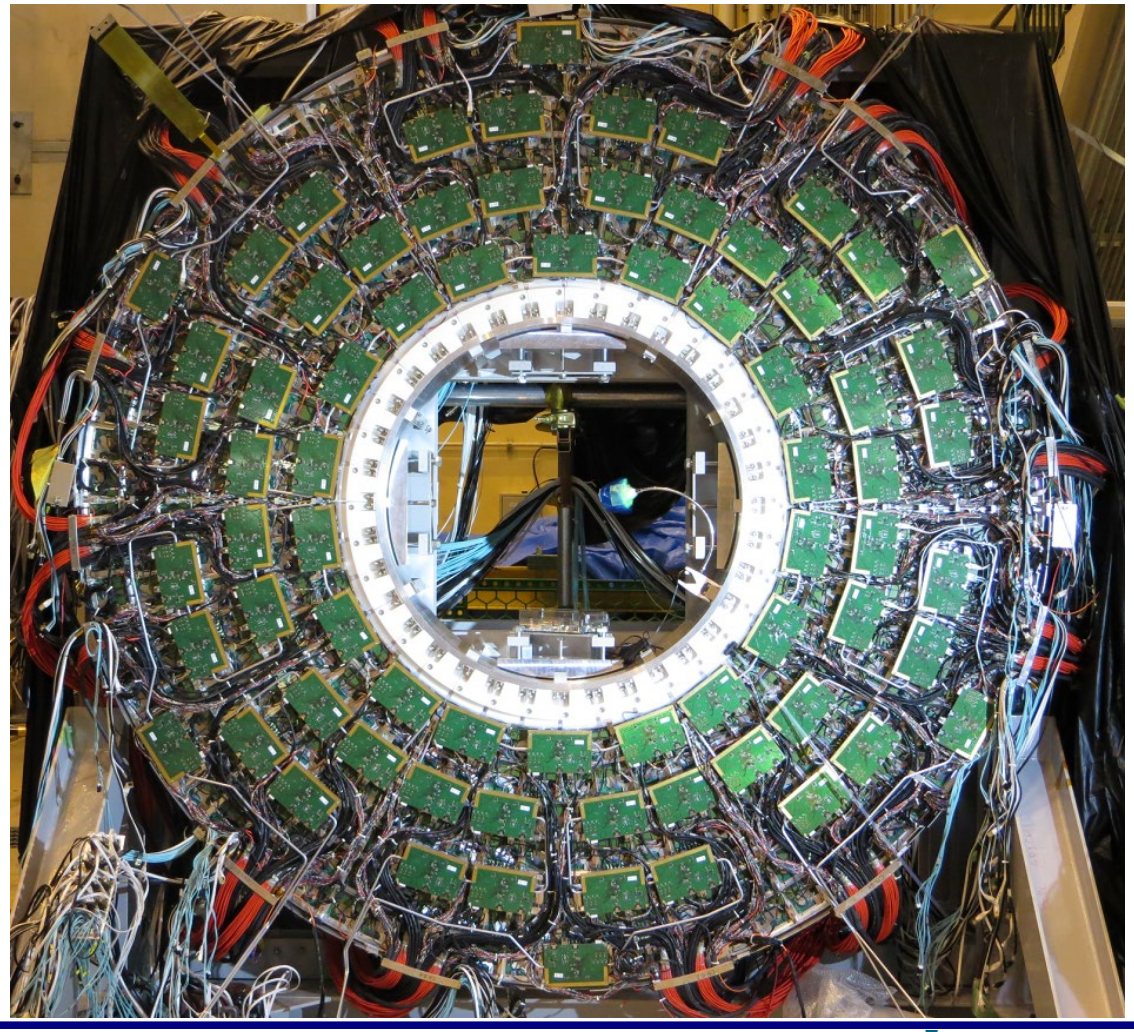

ARICH installation

- Transfer of the forward end-cap to final position in 2017, first beam operation of Belle II April – June 2018
- Extracted and reinstalled during 2018 shutdown for cooling system upgrade before the beam operation start in 2019

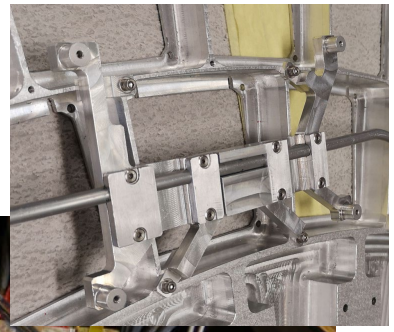

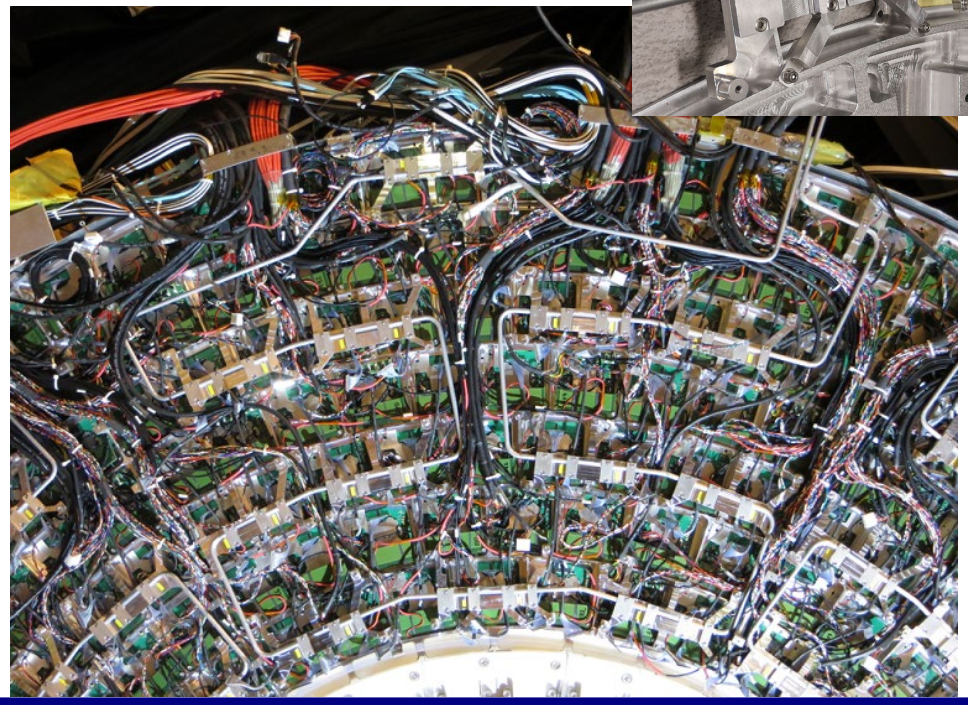

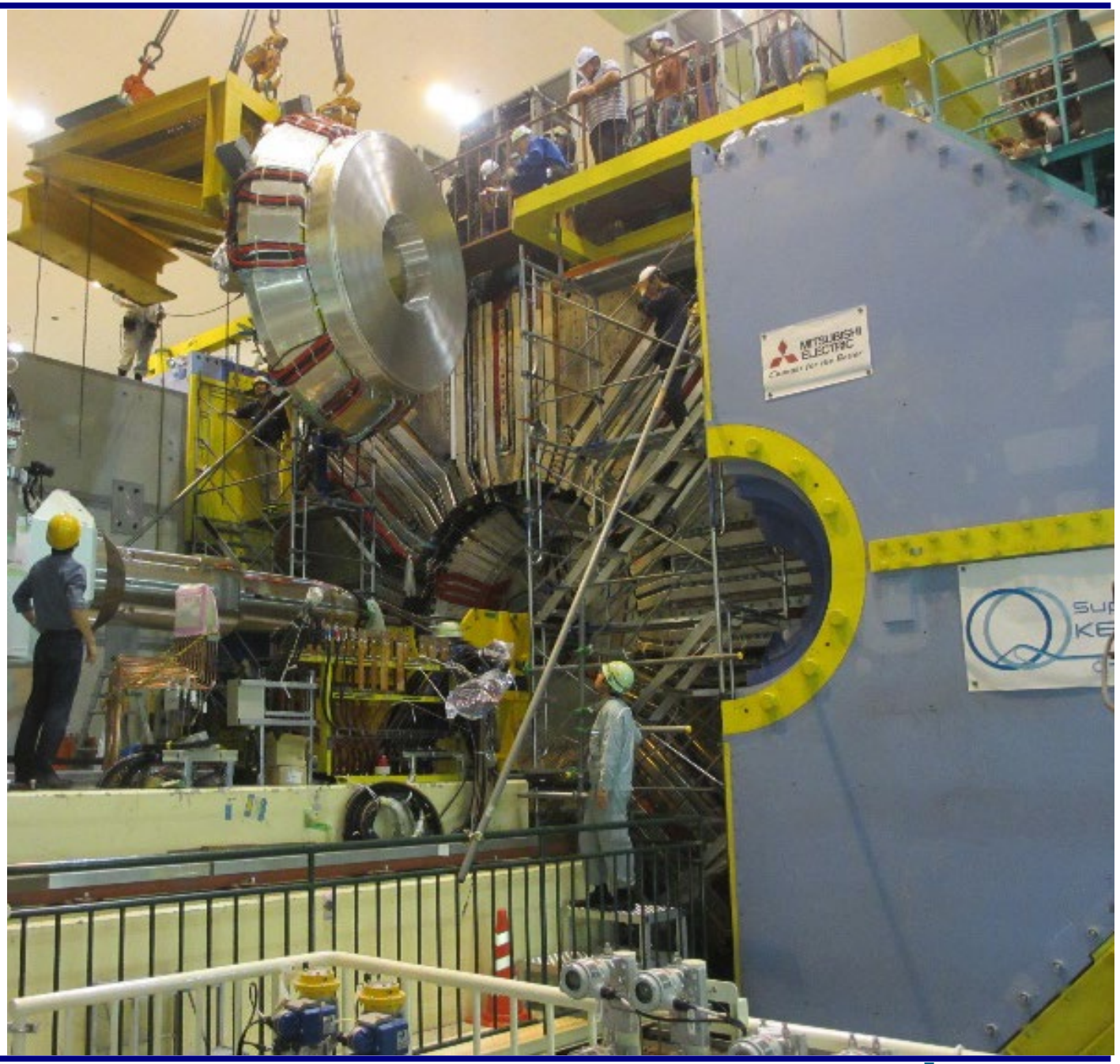

ARICH operation status before LS1

Since March 2019 ARICH is fully operational.

- Current status:
  - ≈ 94 % of ARICH channels operational
  - ≈ 1 %, 1 merger group with 5 HAPD modules, off due to LV cable problem
  - ≈ 5 %, off due to HV or bias problems – different reasons under study
- Electronics efficiency for single photon signals well above 90% – threshold set at 50 mV.

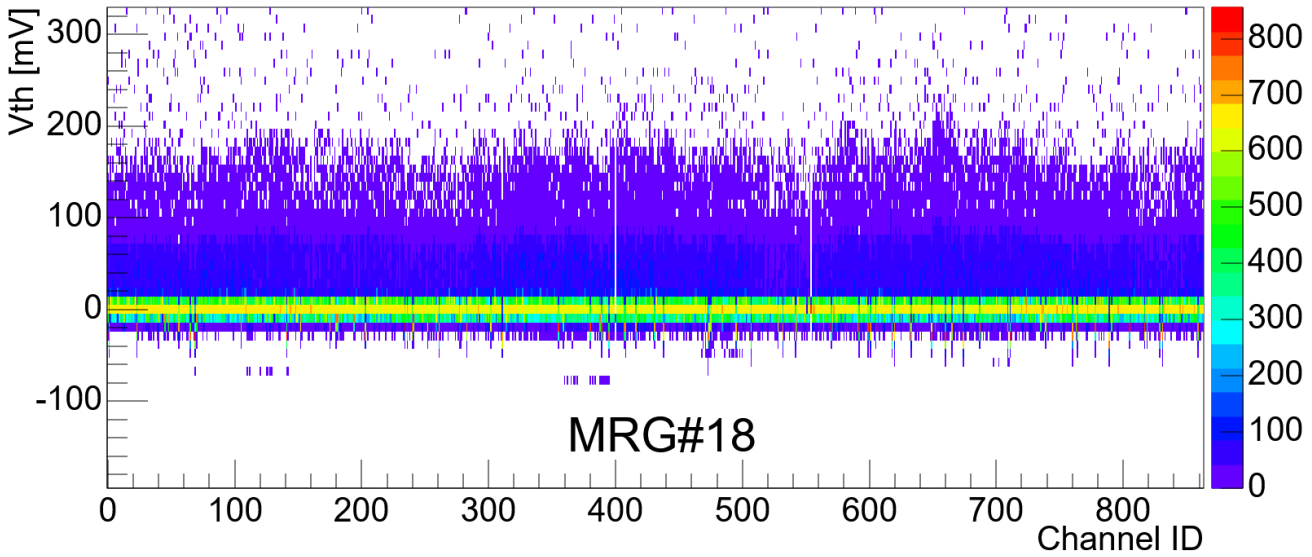

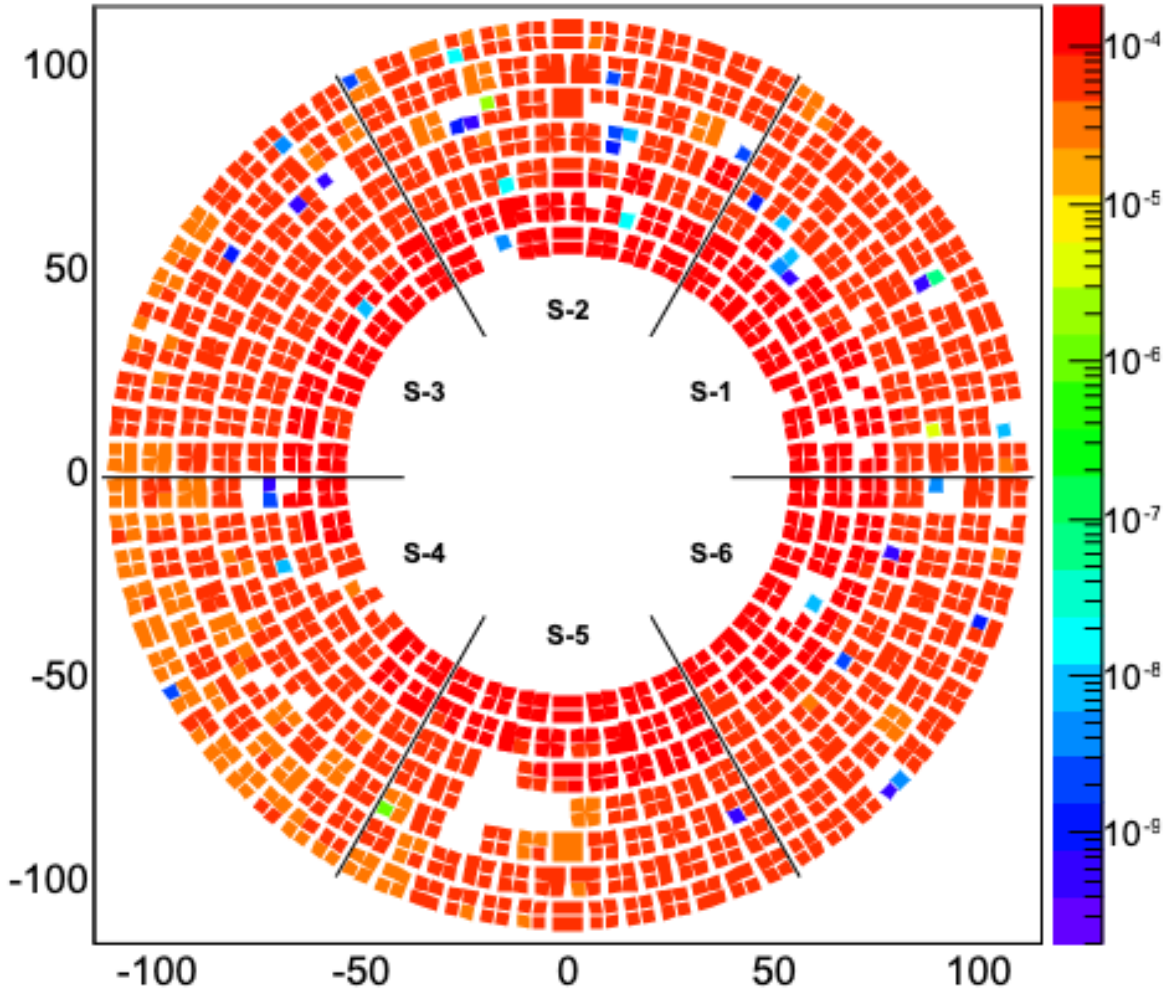

- Average hits per APD per event – white, blue, green are inactive APDs

- Threshold scan for all the channels connected to merger 18 - LED illumination

HAPD leakage current - fluence

Neutron fluence estimate:

- Average increase of leakage current $\approx 400\ nA/APD$ ($30\ nA \rightarrow \approx 10^9 \frac{n_{eq}}{cm^2}$)
- fluence estimate: $\Delta I_b \approx 450\ nA \rightarrow \approx 1.5 \cdot 10^{10} \frac{n_{eq}}{cm^2}$ → more than one order below total expected from simulation
- expected to operate at least up to $10^{12} \frac{n_{eq}}{cm^2}$

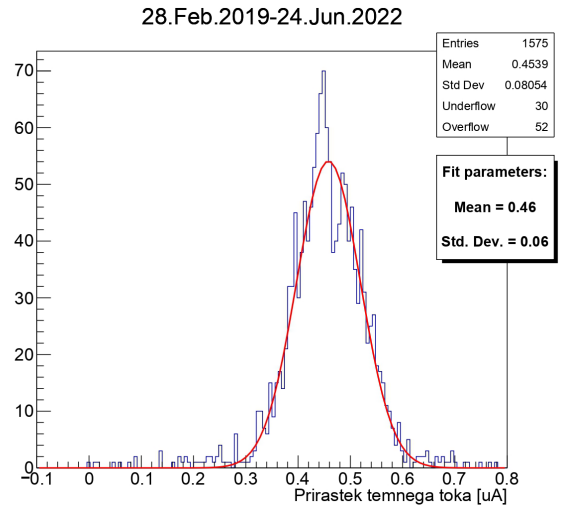

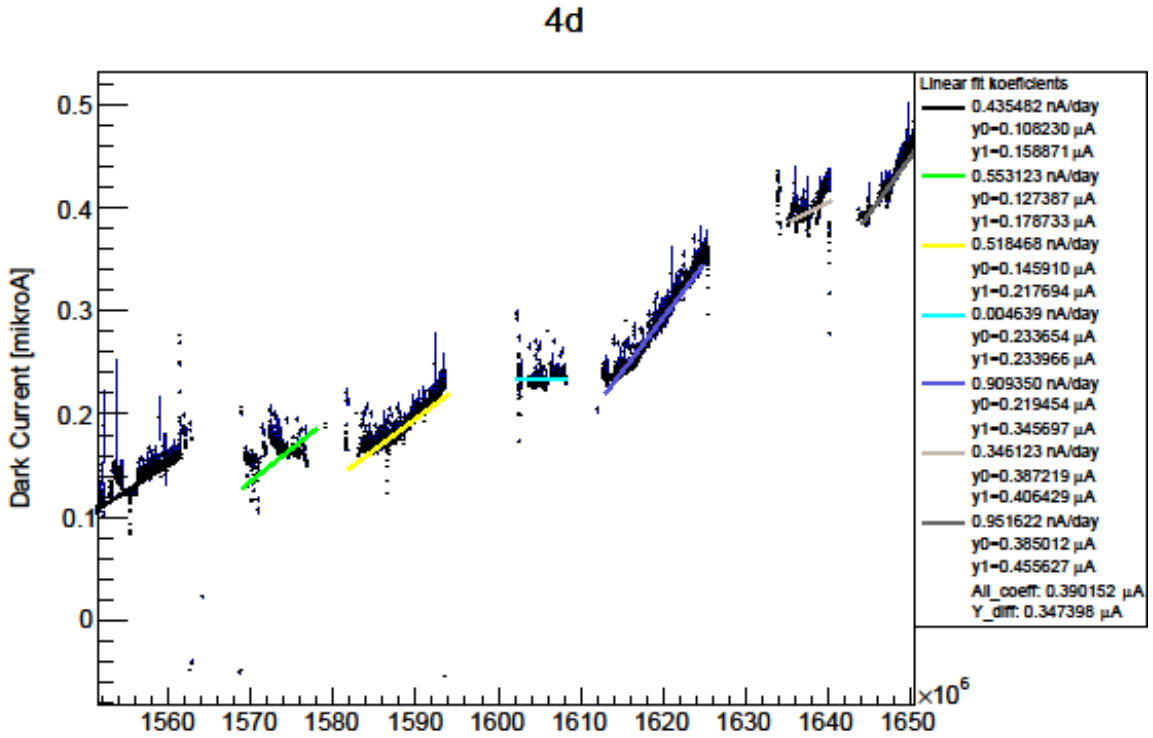

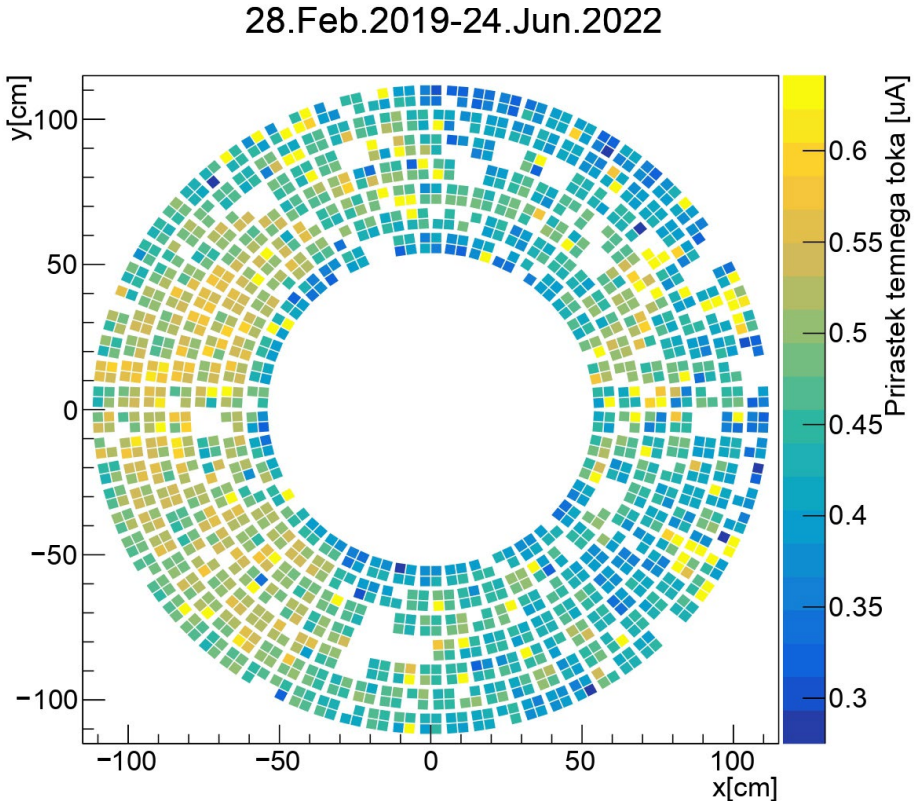

ARICH calibration and alignment ($e^+e^- \to \mu^+\mu^-$)

- First, detector efficiency is calibrated by identifying and removing hot and dead channels.
- ARICH is aligned by maximising the agreement between expected and measured photon distributions and includes:
  - global alignment to tracking system
  - internal alignment of positions and rotations of mirrors and aerogel tiles
- After alignment, a very good agreement is achieved between expected and measured Cherenkov angle distributions.

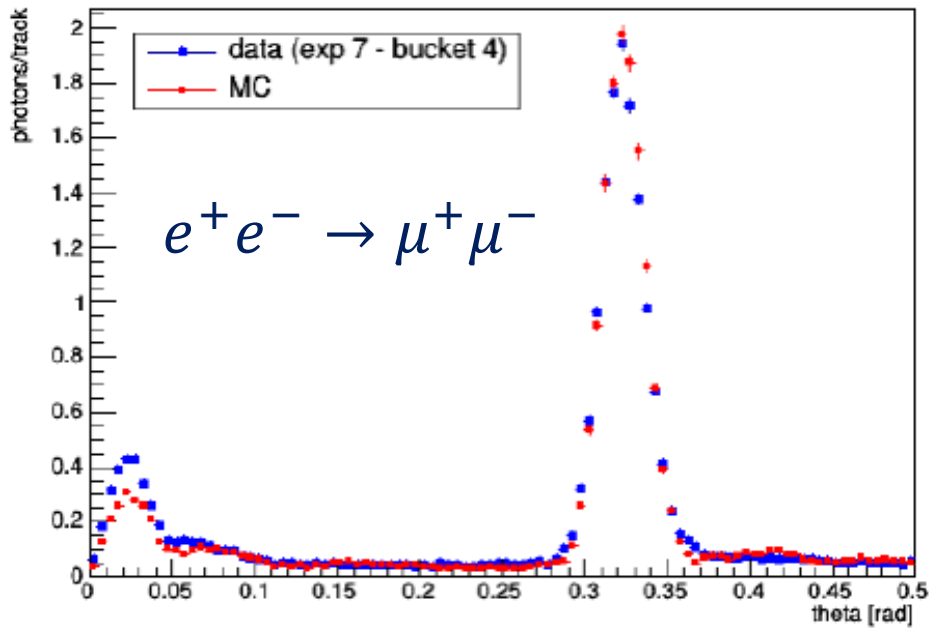

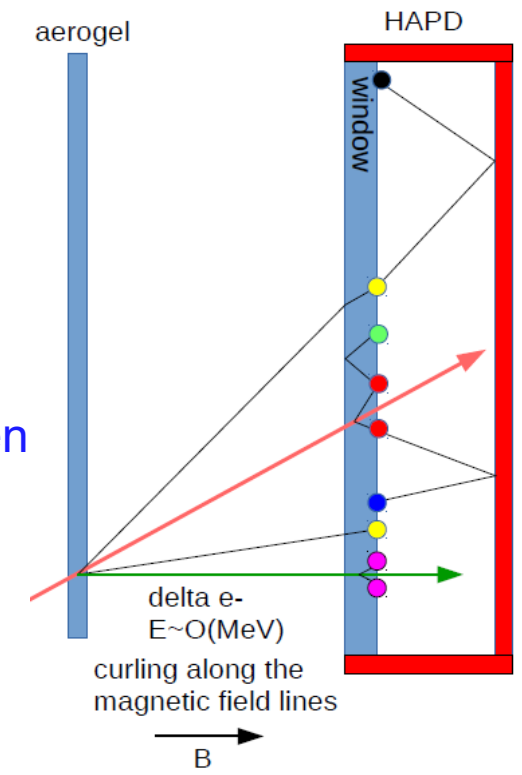

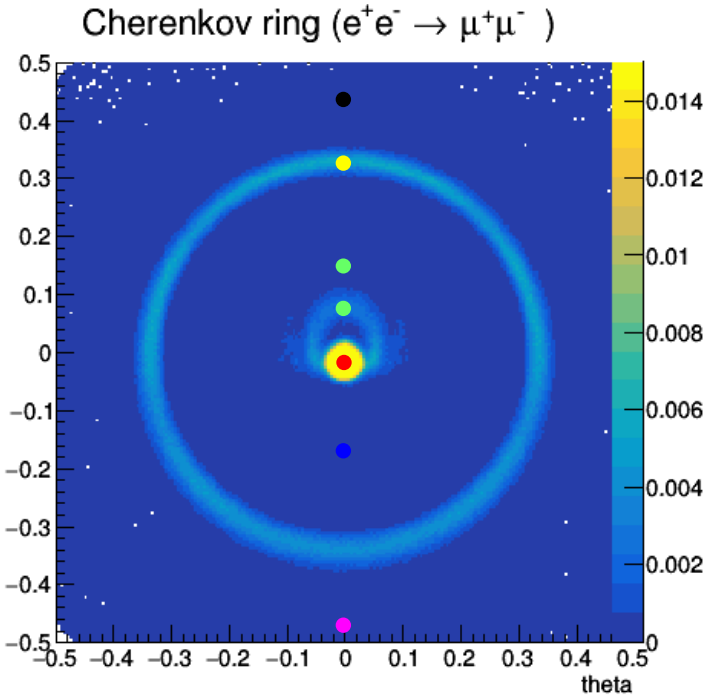

Photon distribution components:

- **Cherenkov photons from aerogel – direct** and scattered
- Cherenkov photons produced in HAPD window:
  - by primary particle
  - by delta electrons from aerogel
- Cherenkov photons from air gap
- All above can undergo further reflections inside HAPD

ARICH calibration and alignment ($e^+e^- \to \mu^+\mu^-$)

- First, detector efficiency is calibrated by identifying and removing hot and dead channels.
- ARICH is aligned by maximising the agreement between expected and measured photon distributions and includes:
  - global alignment to tracking system
  - internal alignment of positions and rotations of mirrors and aerogel tiles
- After alignment, a very good agreement is achieved between expected and measured Cherenkov angle distributions.

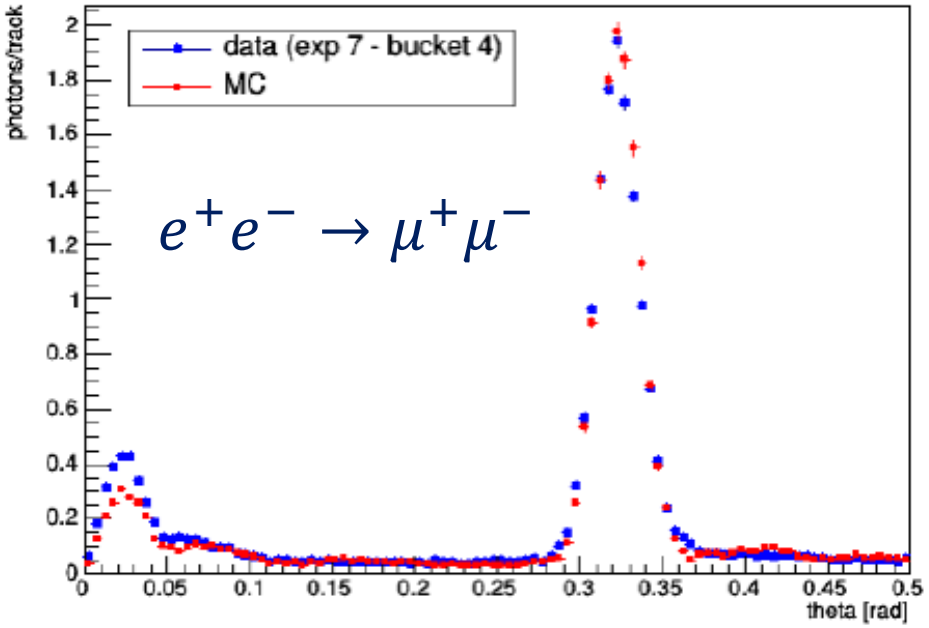

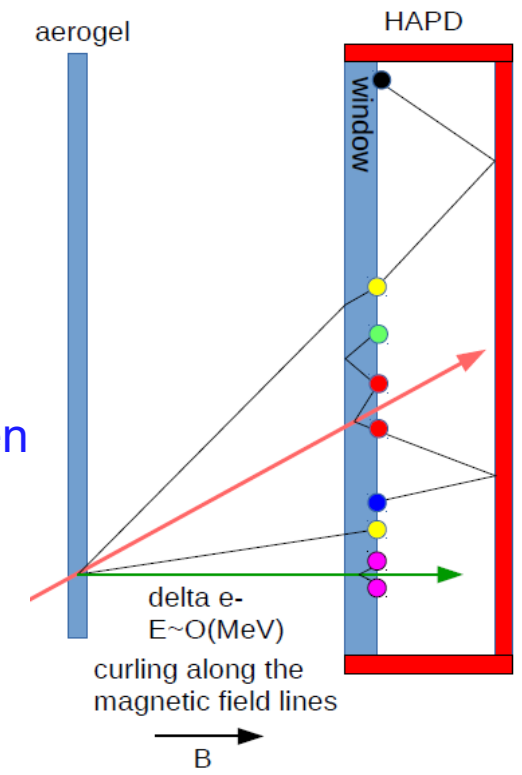

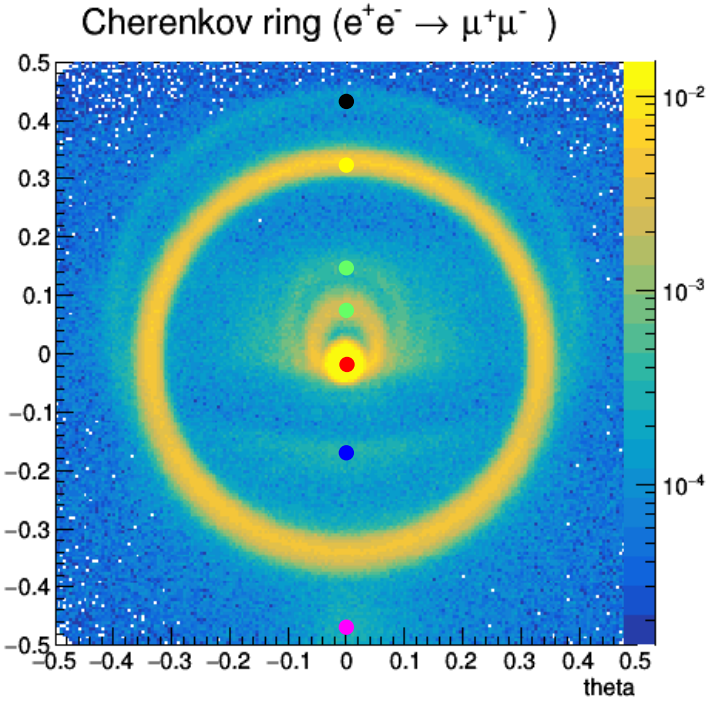

Photon distribution components:

- **Cherenkov photons from aerogel – direct** and scattered
- Cherenkov photons produced in HAPD window:
  - by primary particle
  - by delta electrons from aerogel
- Cherenkov photons from air gap
- All above can undergo further reflections inside HAPD

ARICH alignment status

- Reconstructed mean Cherenkov angle shows a systematic deviation from expectation at inner and outer edge of ARICH acceptance and for some tiles in the second ring.
- This has been compensated by the alignment of the aerogel tiles.

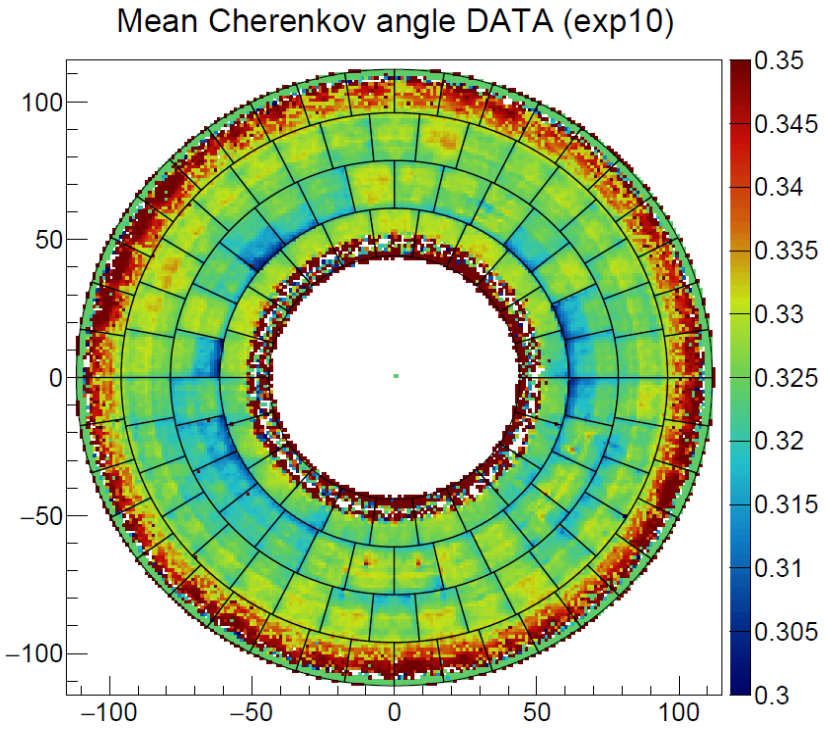

- Shifts away from the photo-detector plain at the inner and outer edge are not yet understood.

- Tilts in the second ring can be understood since the tiles are fixed with longer strings spanning the first and the second ring. Inner edges of some tiles might have shifted toward the photodetector plain during the ARICH movements.

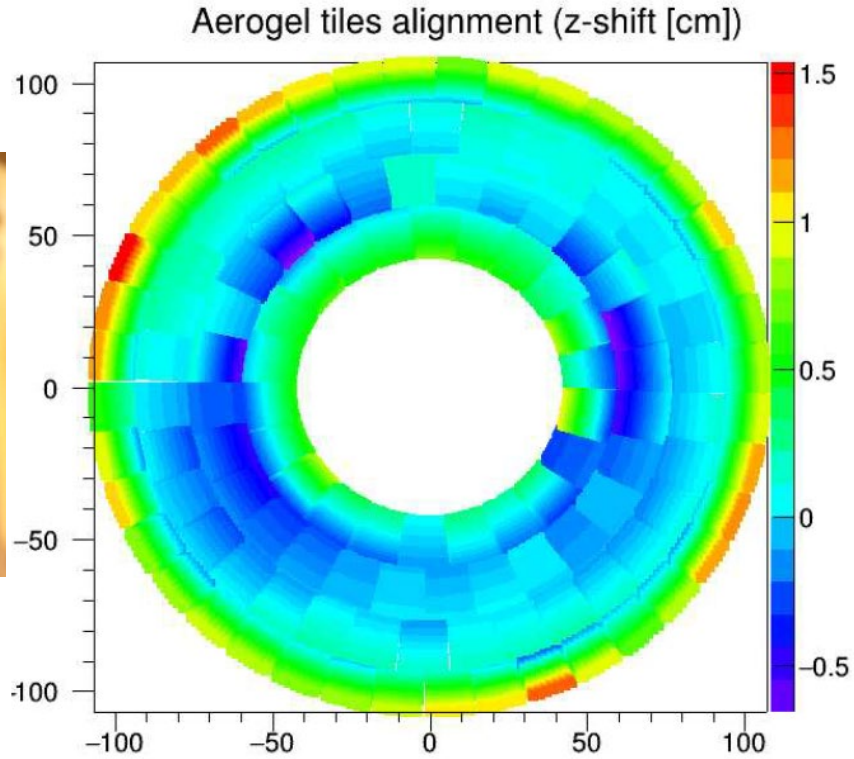

Cherenkov angle for μ^+ μ^-

- Variation of the mean Cherenkov angle at the outer aerogel ring for mu-mu events.

- Both, positive and negative muons, show the same variation of mean Ch. angle while deviation observed in MC is negligible.

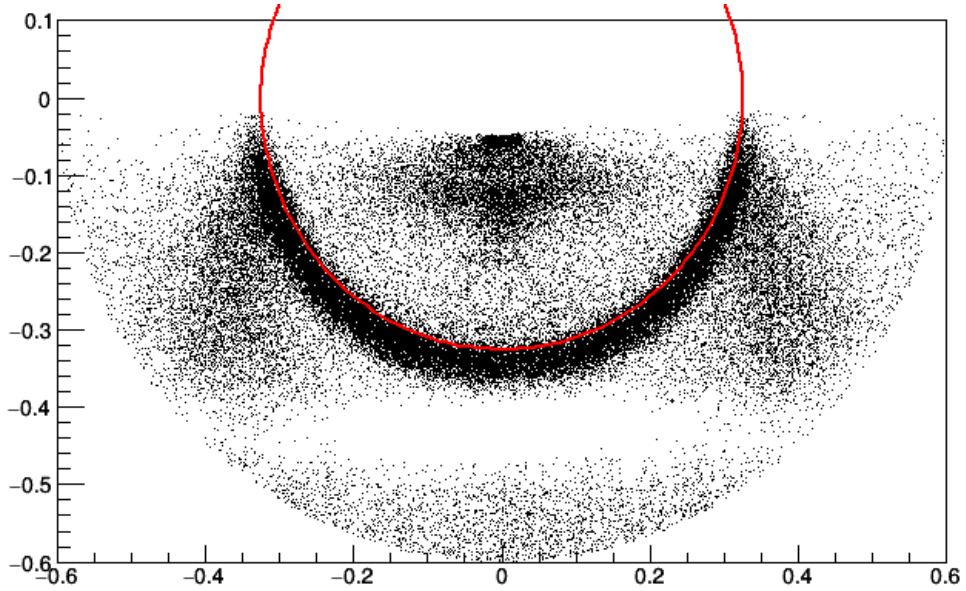

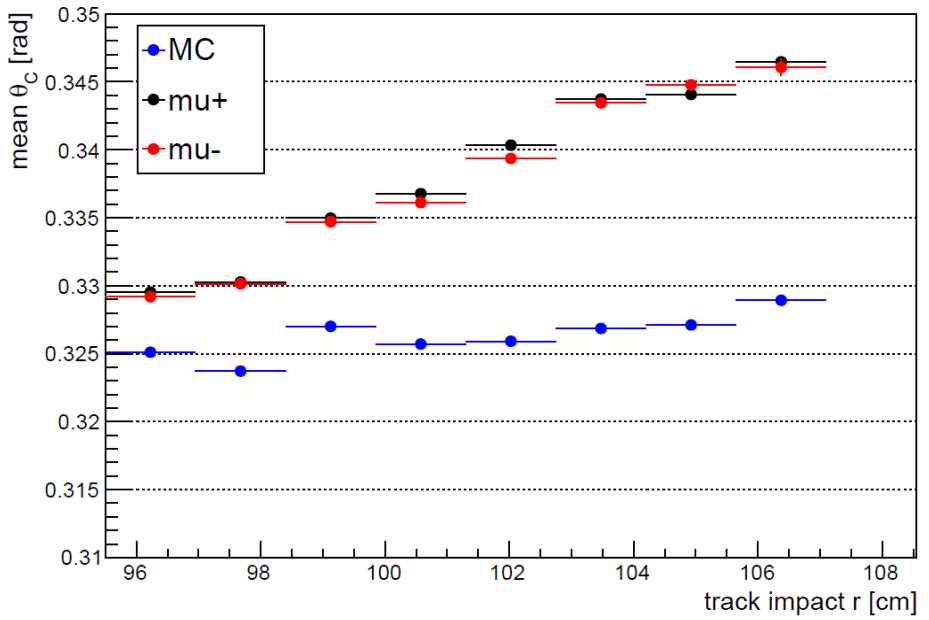

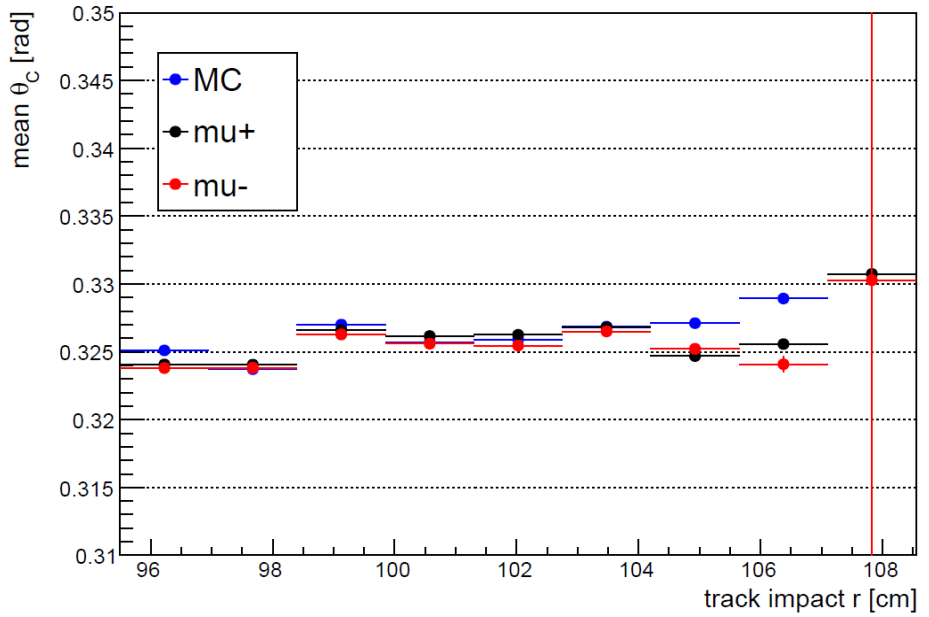

- After alignment of the aerogel tiles, data and MC are compatible.

Likelihood function and PDF construction

- PID is based on a maximum likelihood function – comparing measured with expected hit distribution for different particle hypothesis

$$\ln \mathcal{L}_h = -N_h + \sum_{hit\ i} \left[n_{h,i} + \ln(1 - e^{-n_{h,i}}) \right]$$

$n_{h,i}$ is the expected number of hits detected by pixel i for hypothesis h - integral of PDF over pixel area, and $N_h = \sum n_{h,i}$

- Main PDF components: direct and scattered Ch. photons from aerogel, correlated and uncorrelated background
- PDF parameters were calibrated by $K_S^0 \to \pi^+\pi^-$ decays for low momentum and $e^+e^- \to \mu^+\mu^-$ for high momentum

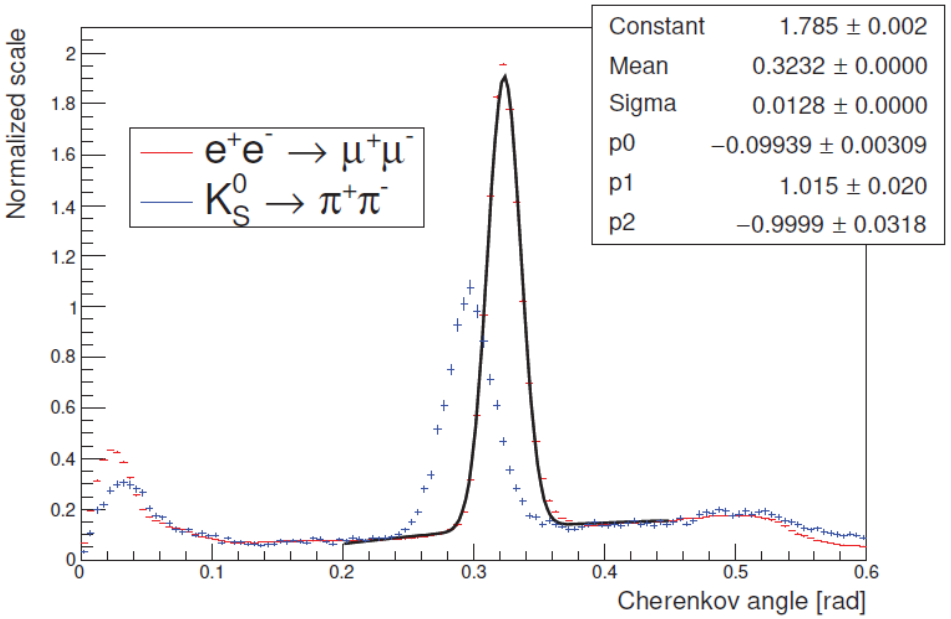

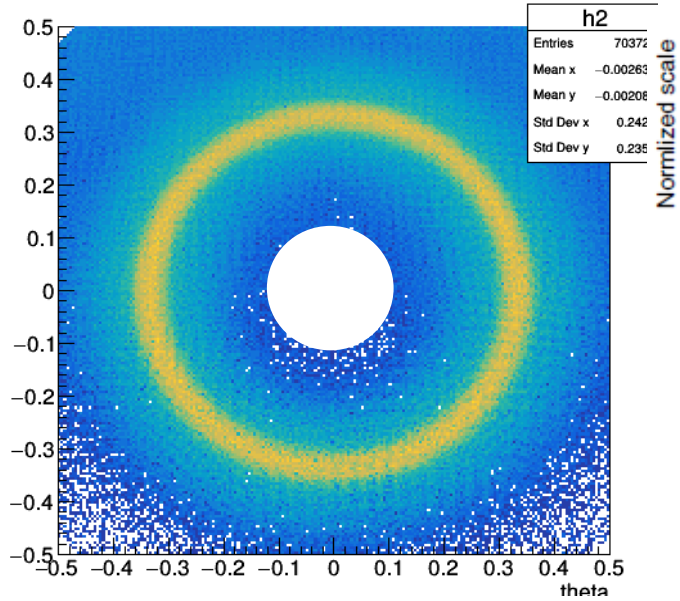

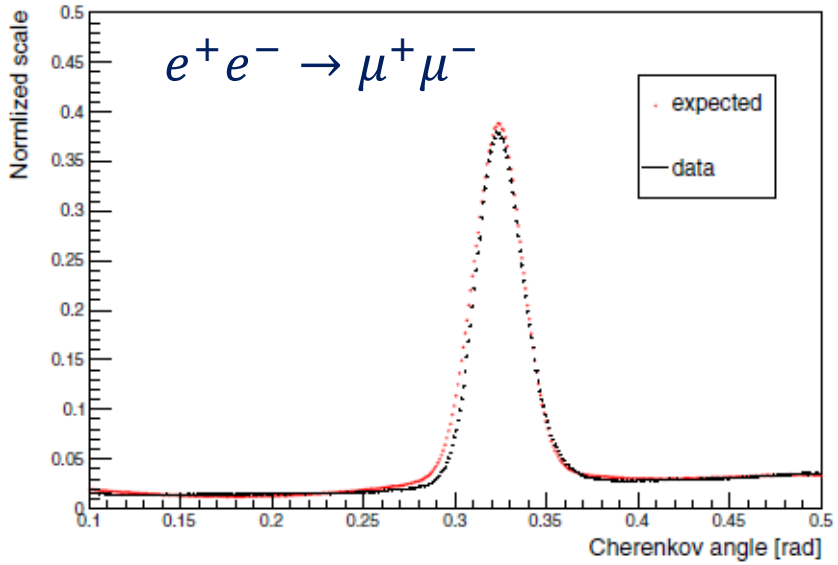

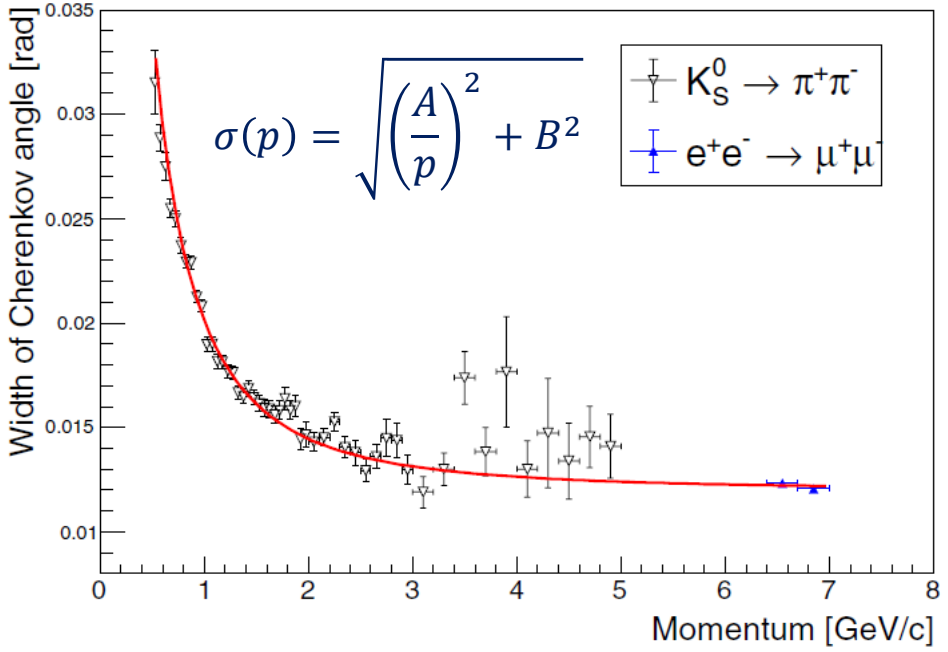

Preliminary results for 2020 data

- ARICH K efficiency vs. π misidentification probability for 2020 data

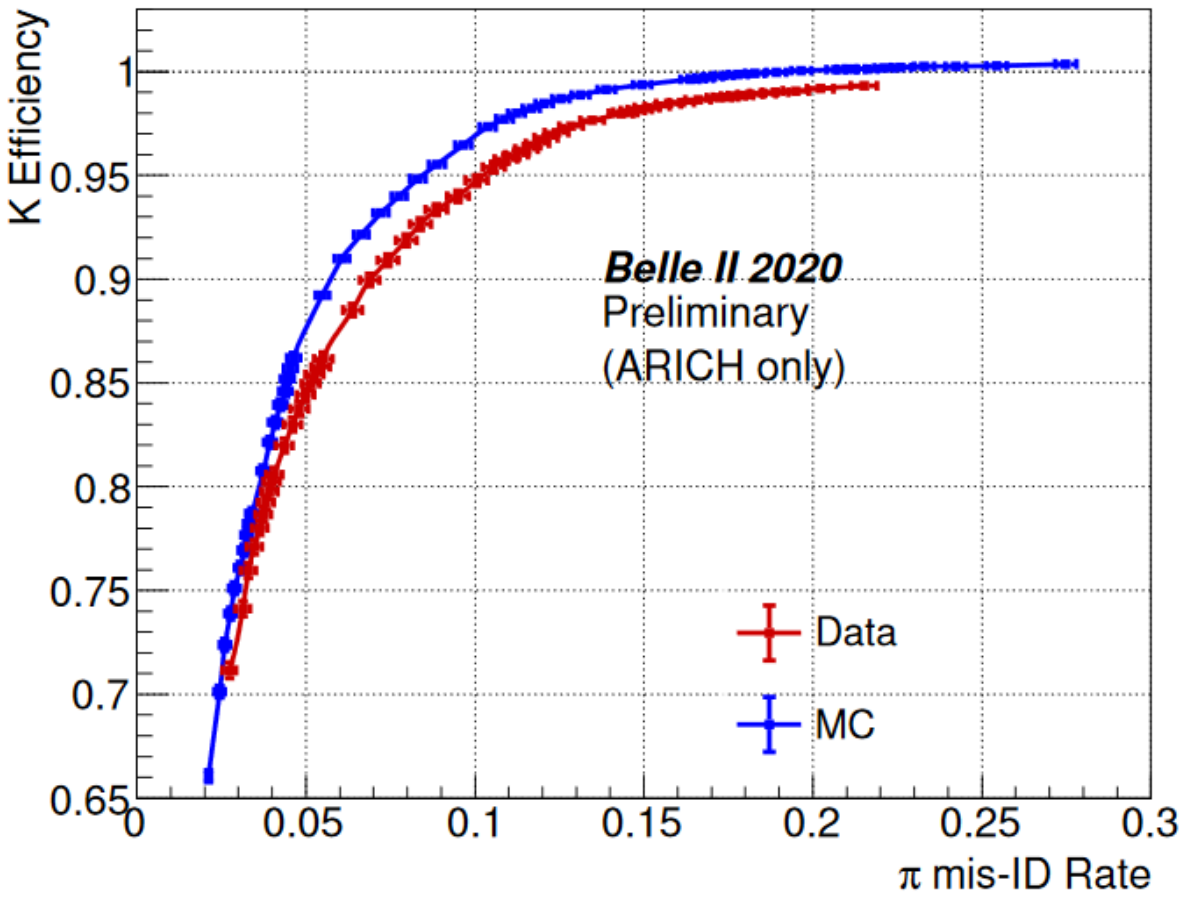

- Momentum dependence of ARICH K efficiency and π misidentification probability for 2020 data

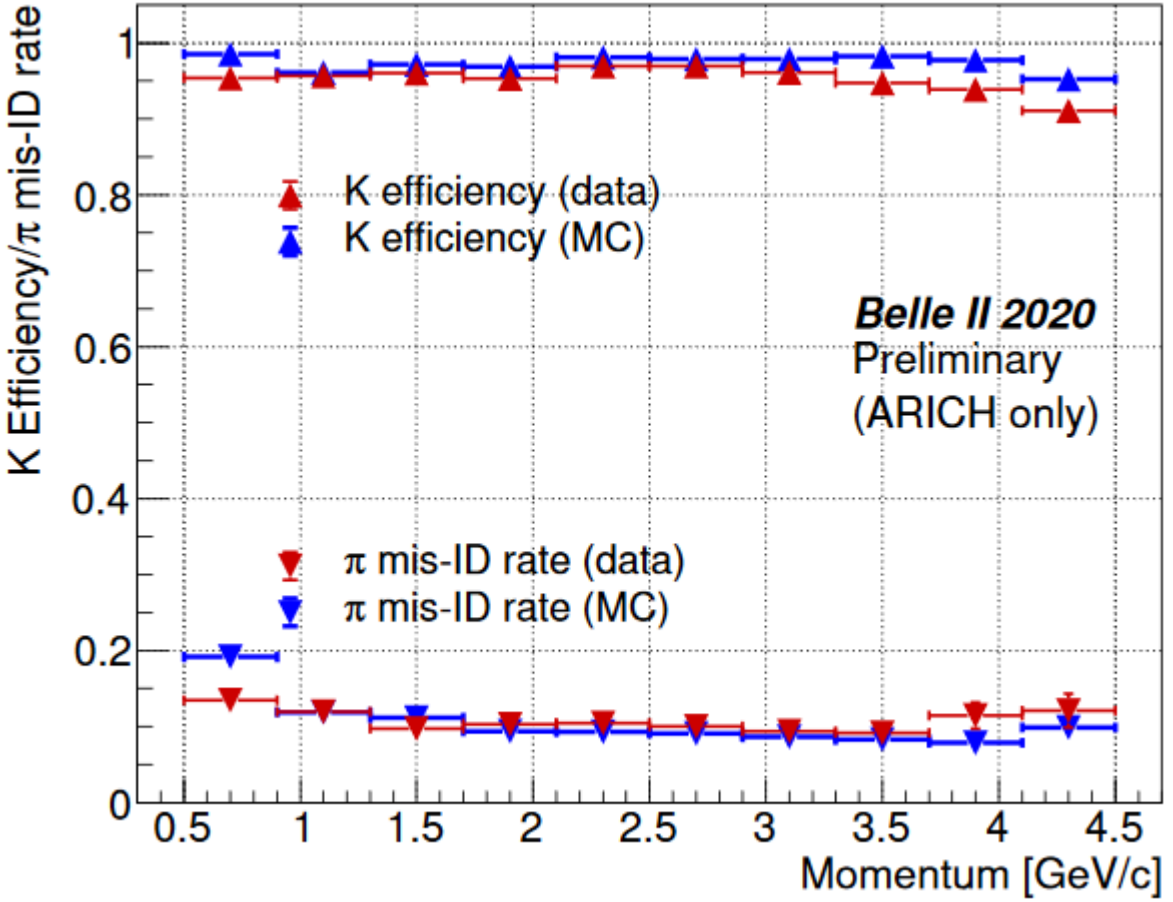

2019a - π/K performance

- Still some disagreement data vs. MC for π on the level of 3% - possible reason: aerogel gap misalignment
- Relatively high π misID – possible reason: tracks with no hit in ARICH (scattered, decayed?)

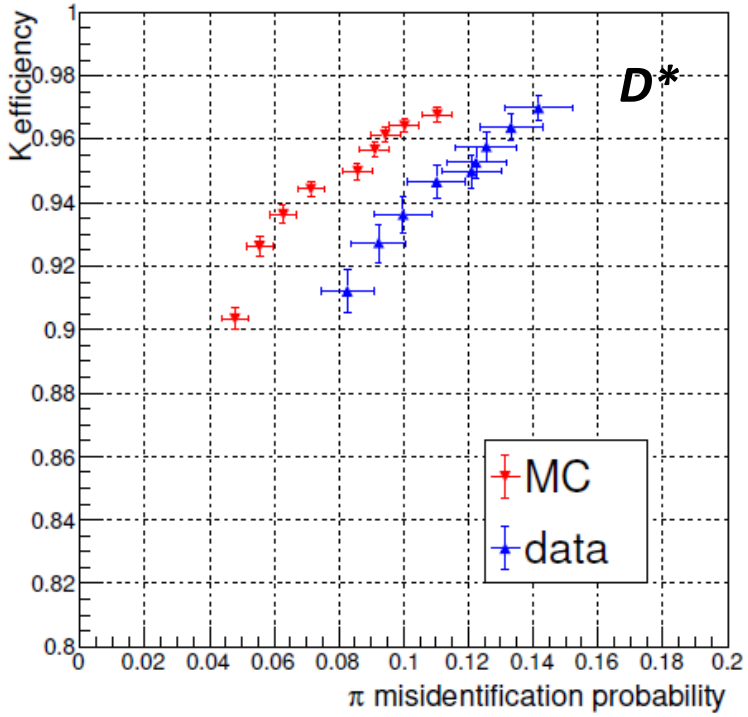

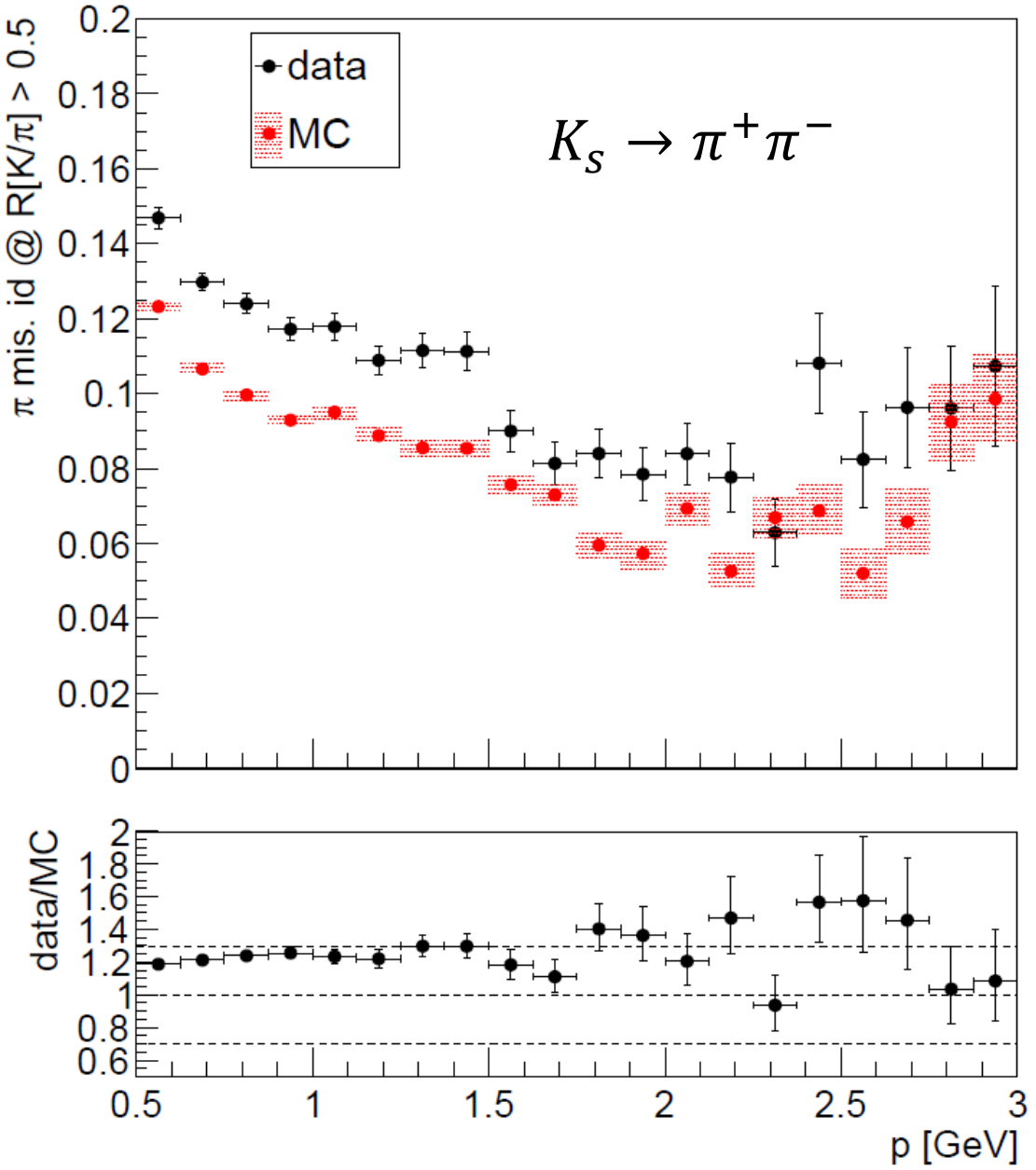

2019a - π MC/data discrepancy

- Check by excluding aerogel tiles edge areas and require associated ECL cluster

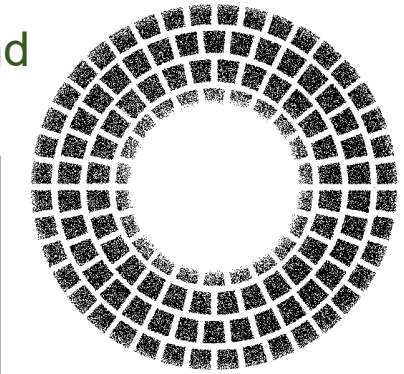

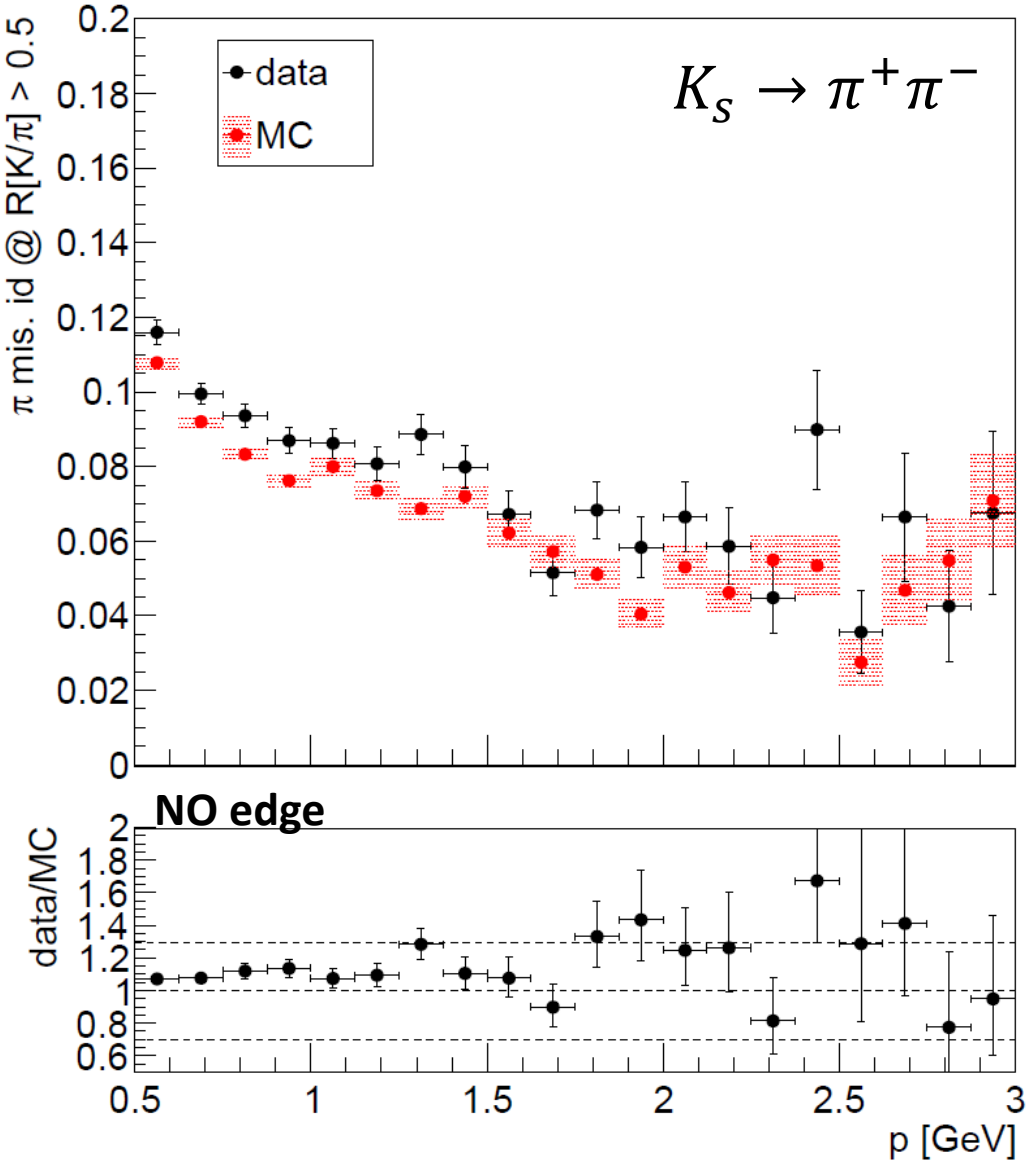

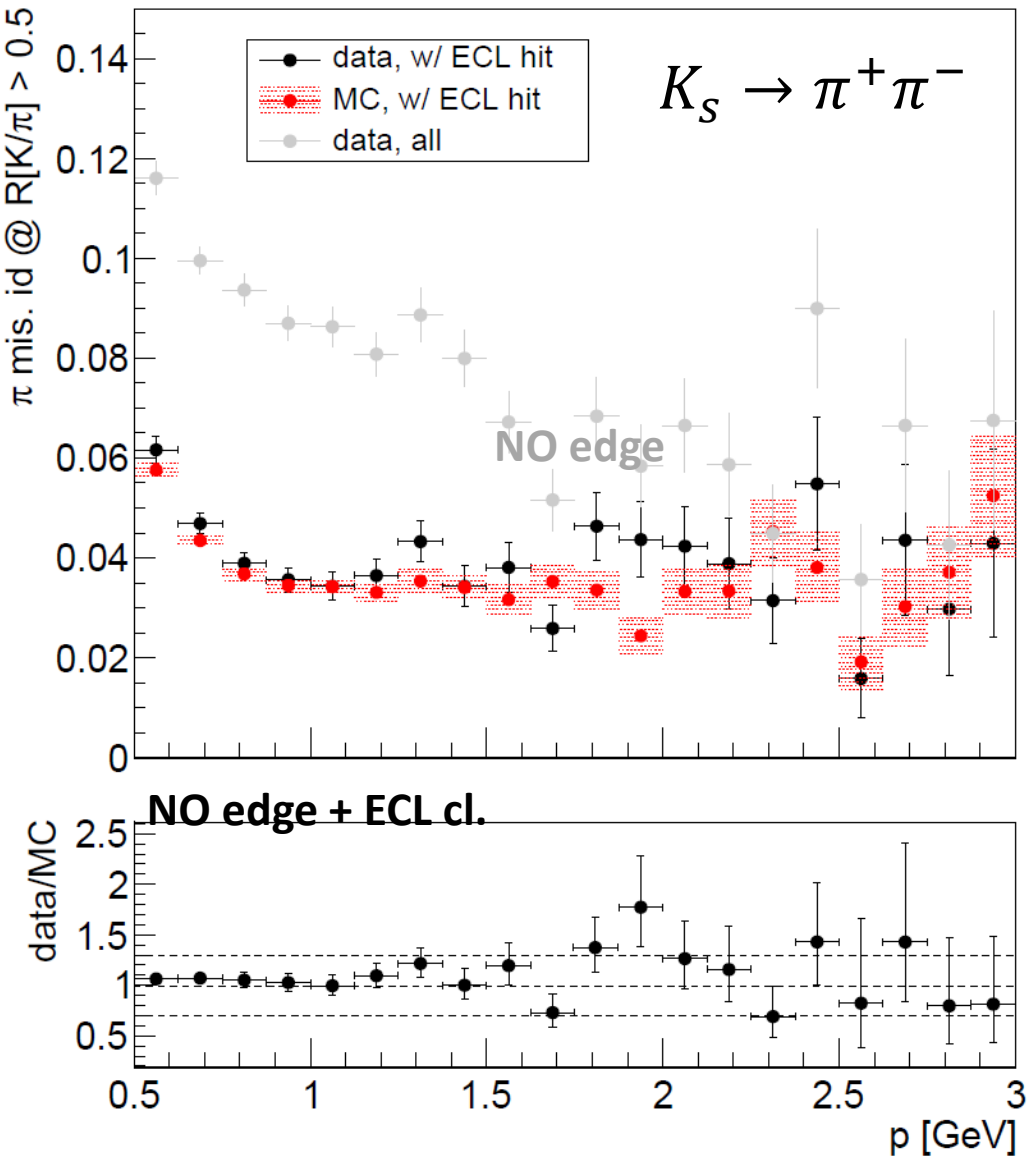

Aerogel tile alignment

- photon loss in the gaps between aerogel tiles taken into account in calculation of expected number of photons for given hypothesis
- misalignment of gap positions (actual vs. assumed) is observed in measured data → increased particle misid. rate

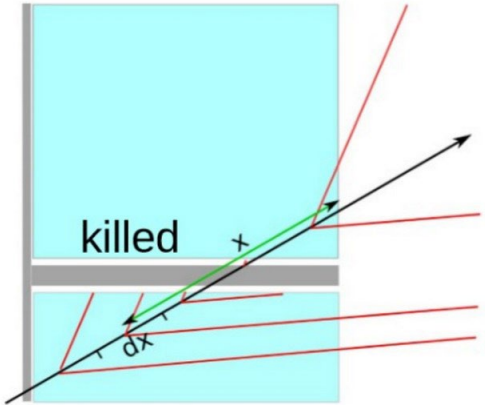

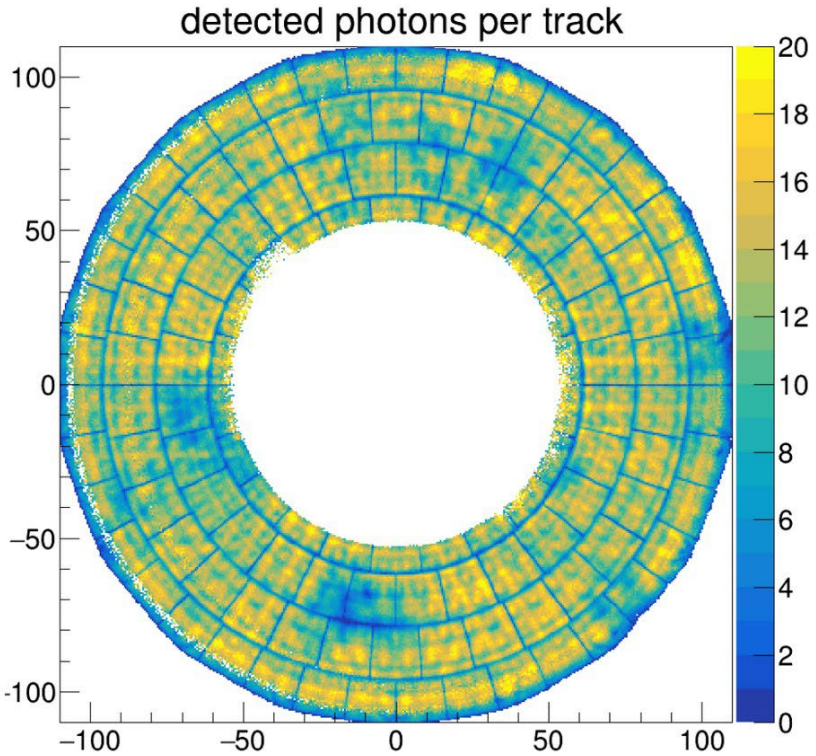

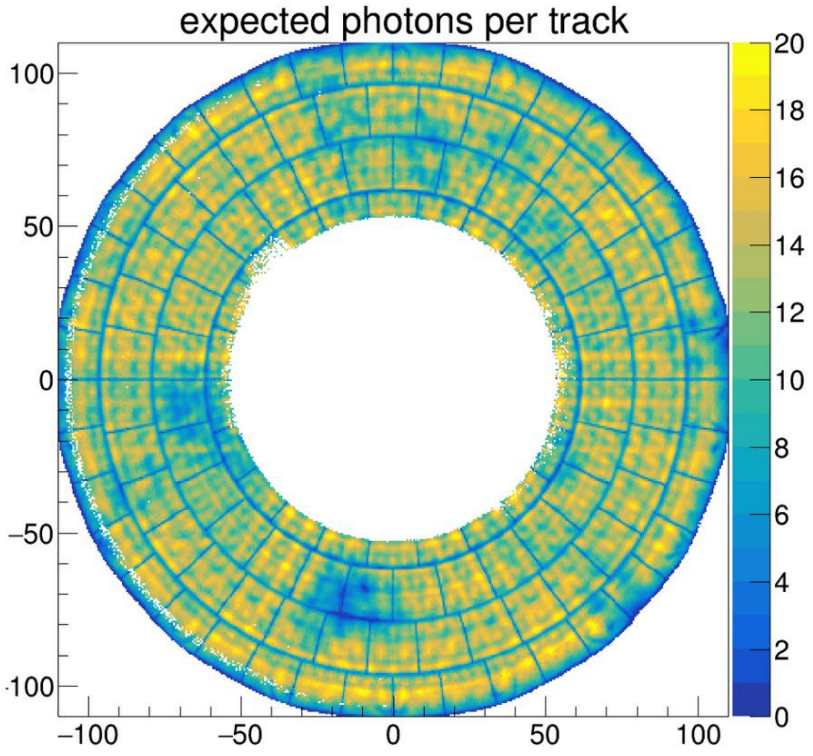

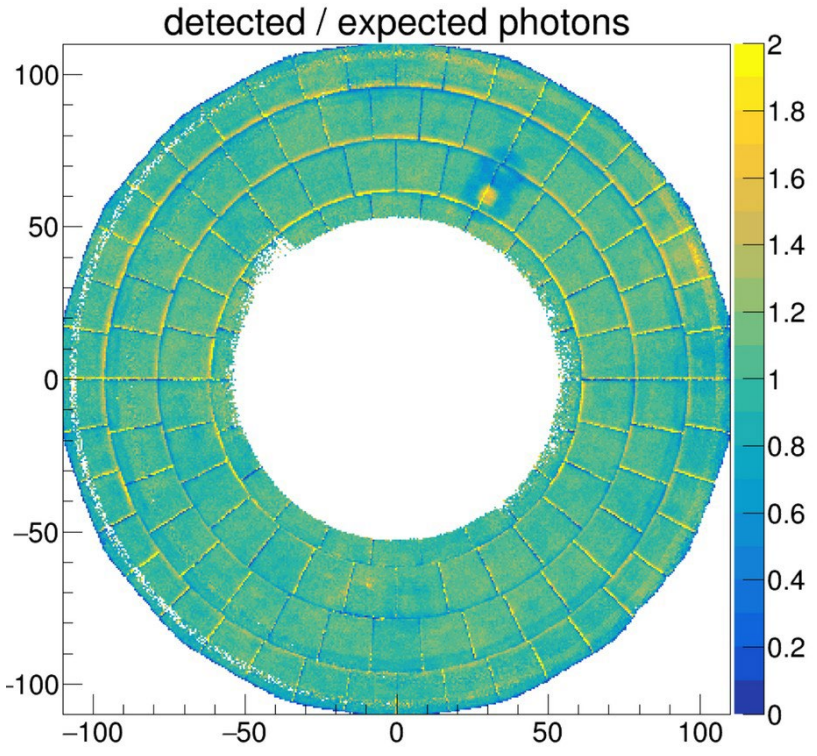

Combined PID – strong scattering/decay

- Large fraction of misidentified pions, especially at low momenta, are due to pions that are strongly scattered or decay on their way to ARICH detector.
- Due to missing photos around extrapolated track position such tracks are likely to be identified as kaons.
- Such tracks can be identified by missing ECL cluster and/or missing signal in case of tracks hit in HAPD window.

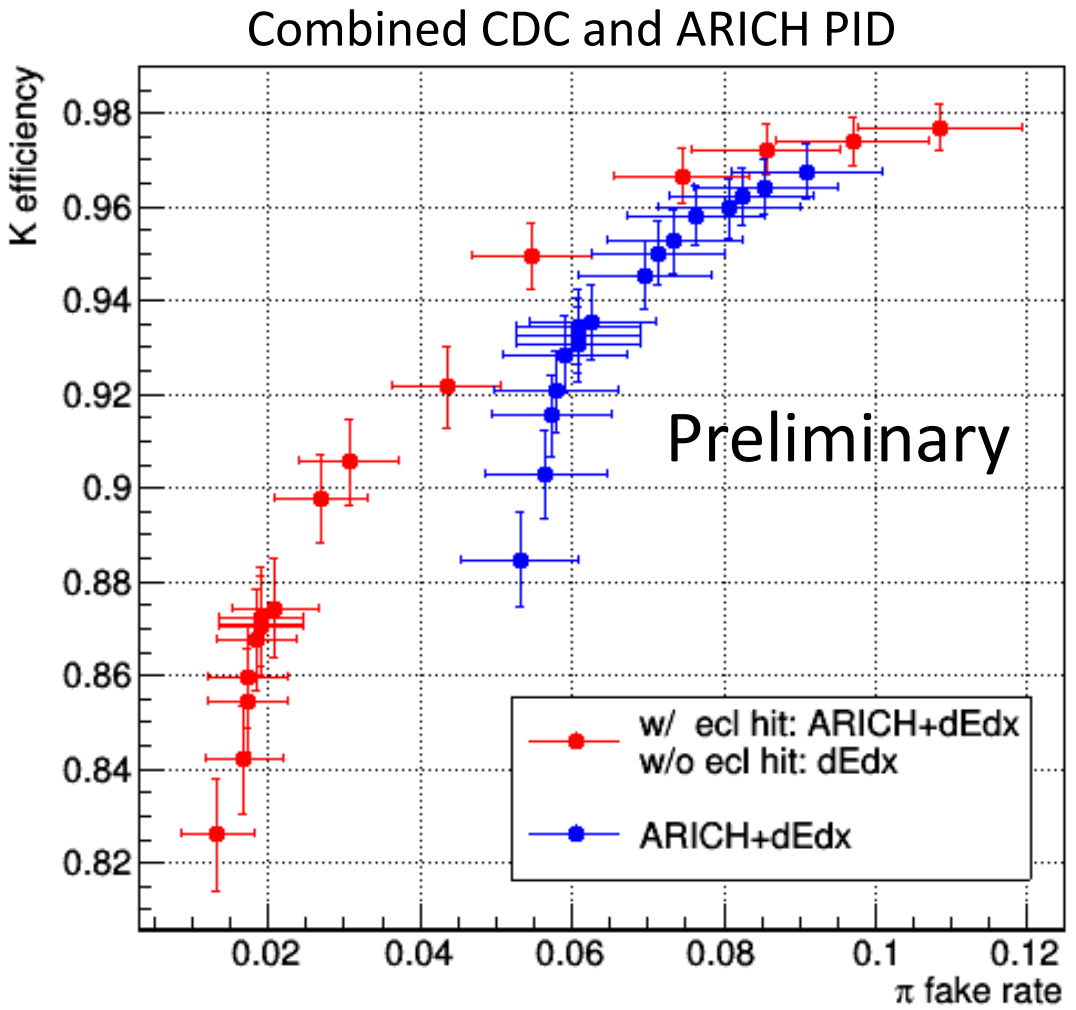

Likelihood PDF improvement

Current PDF

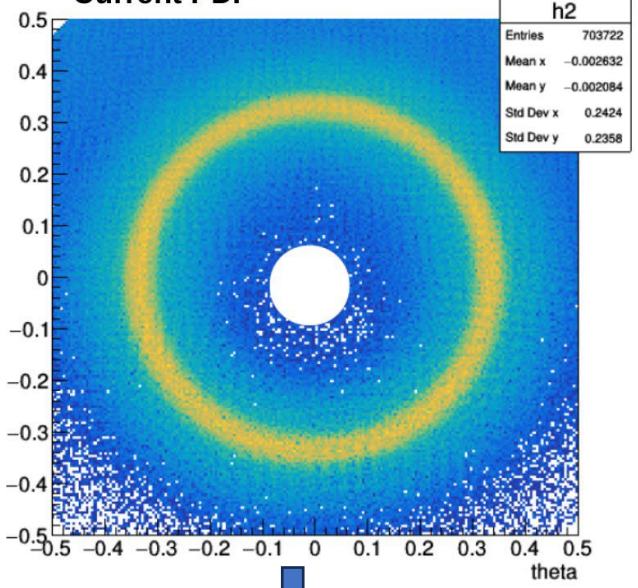

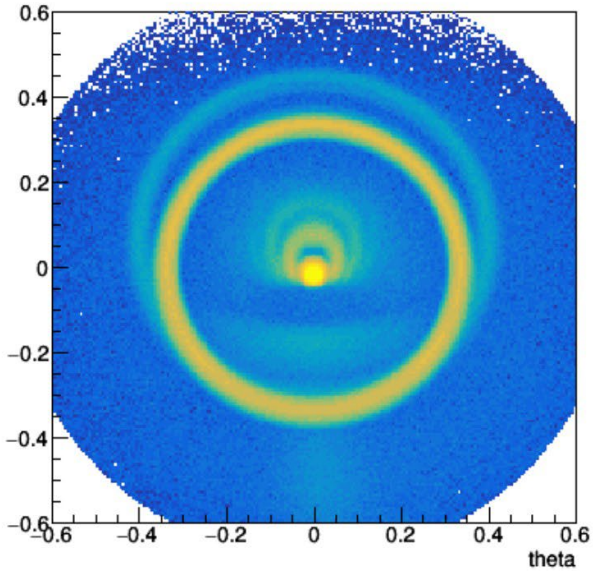

Muons @ ~6.8 GeV

MC

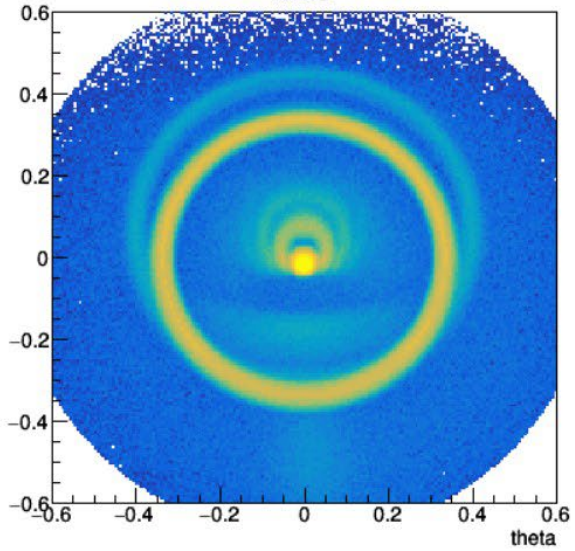

PDF

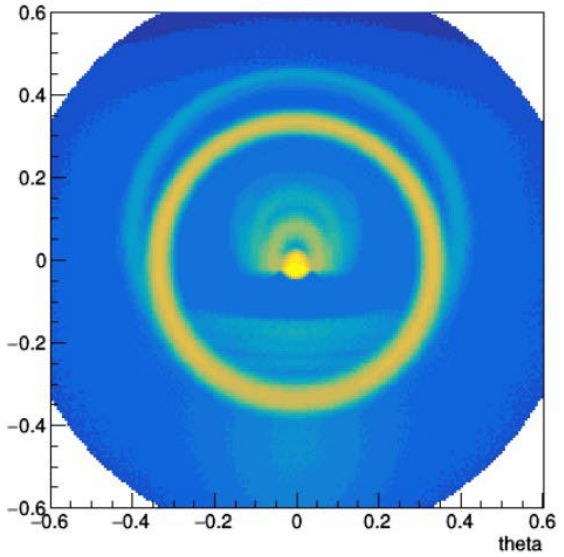

- Small improvement in PID performance

Muons @ 0.5 GeV

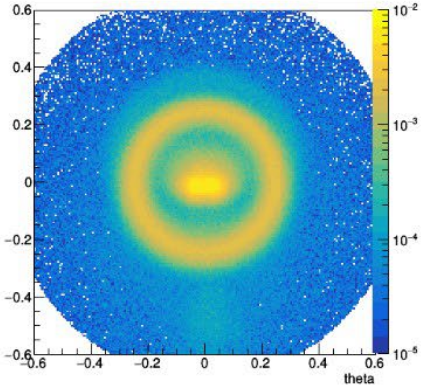

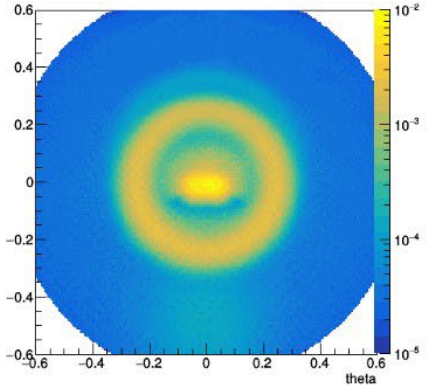

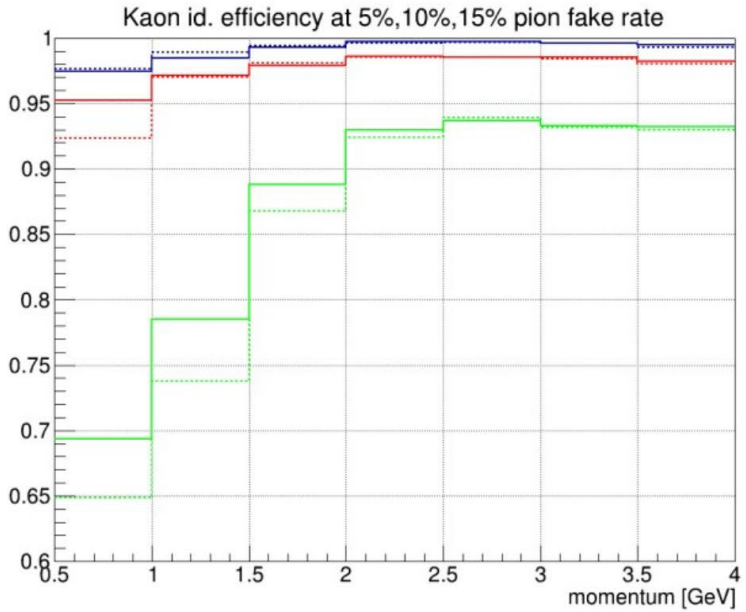

BACKUP SLIDES

2019a – threshold efficiency

- Efficiency for the ~95% channels was estimated by evaluating threshold scans made during LED illumination
- Average efficiency was 88.5% with most of the channels well above 90%

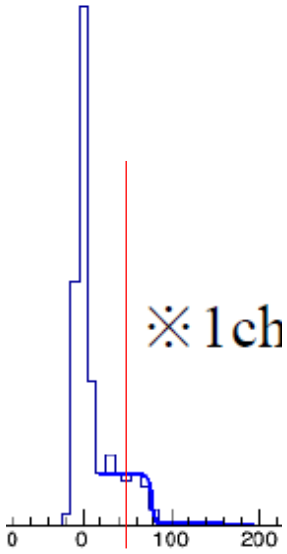

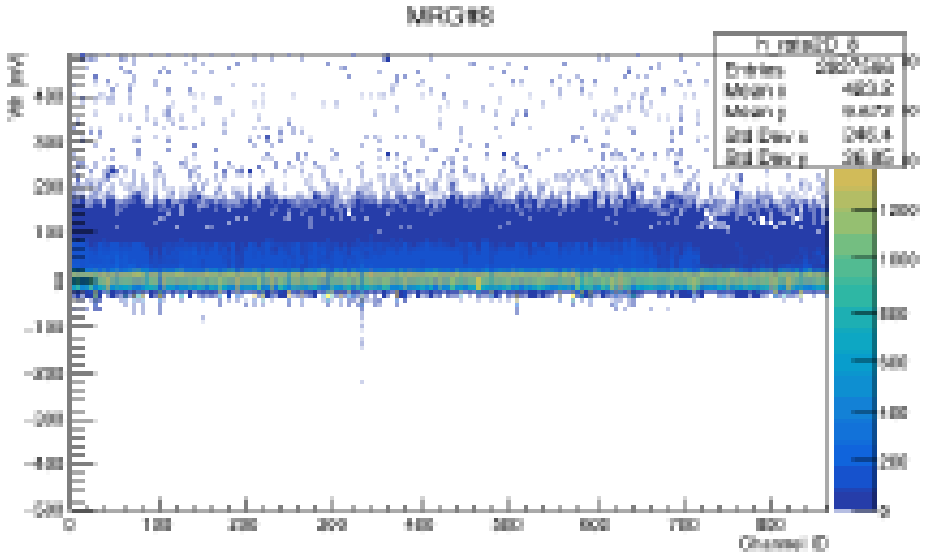

After some channels(APDs) are masked

Efficiency (Vth=50mV)

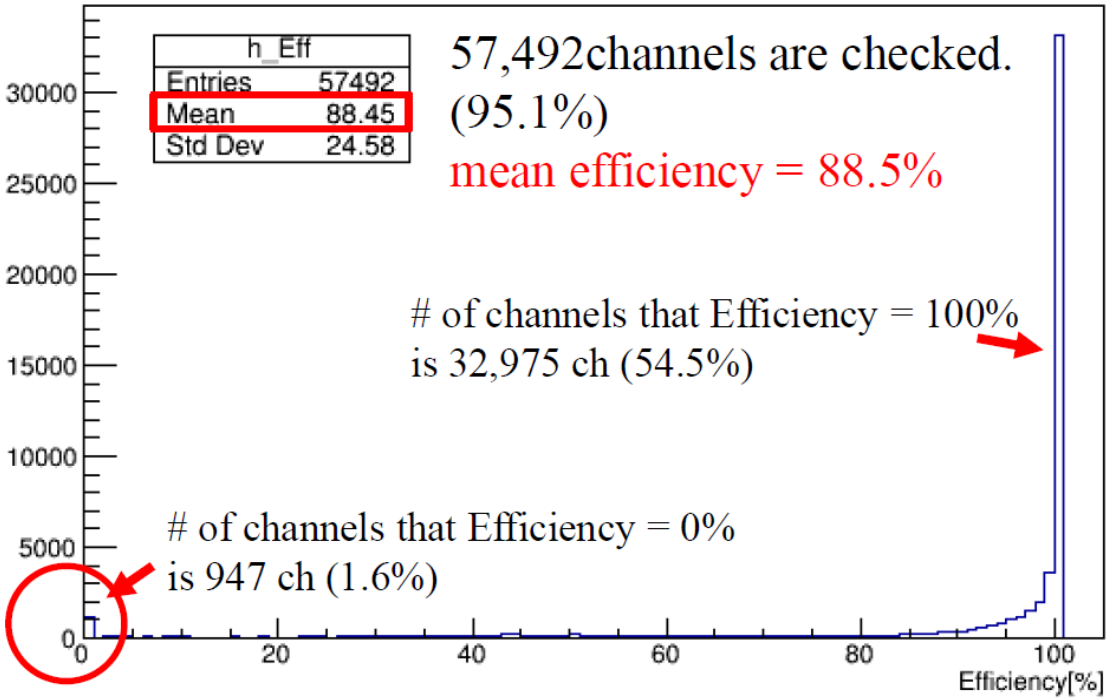

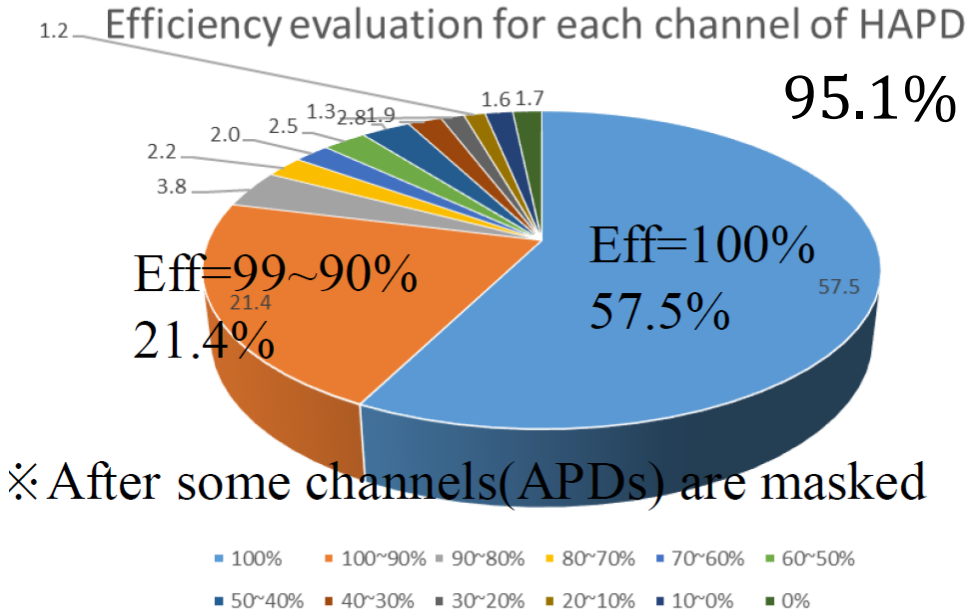

PID performance - $D^{*+} \to D^0\pi^+(D^0 \to K^-\pi^+)$

- π and K identified by the charge of „slow“ π and charge of the track, without using PID
- K/π selection criteria $R_{K/\pi} = \frac{\mathcal{L}_K}{\mathcal{L}_K+\mathcal{L}_\pi}$

	K eff.	π mis.	π eff.	K mis.
Data	$93.5 \pm 0.6\,\%$	$10.9 \pm 0.9\,\%$	$87.5 \pm 0.9\,\%$	$5.6 \pm 0.3\,\%$
MC	$96.7 \pm 0.2\,\%$	$7.9 \pm 0.4\,\%$	$91.3 \pm 0.3\,\%$	$3.4 \pm 0.4\,\%$

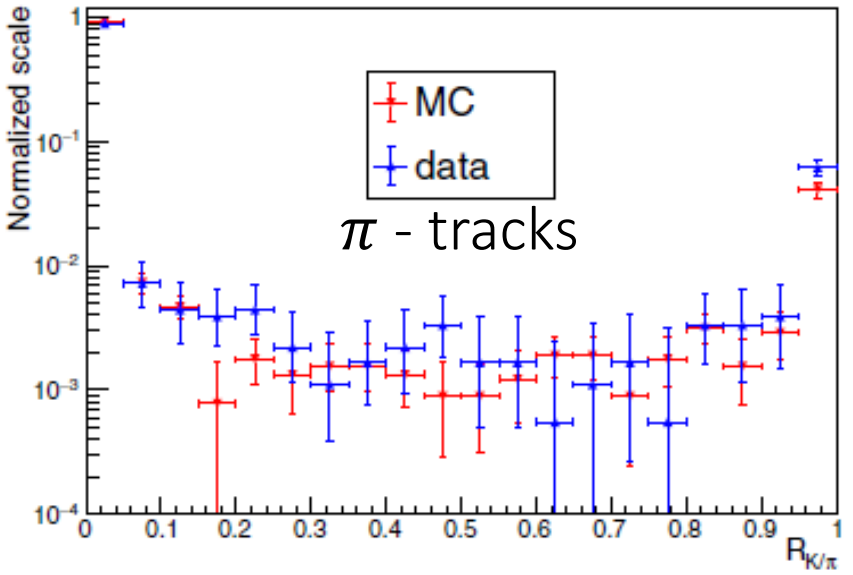

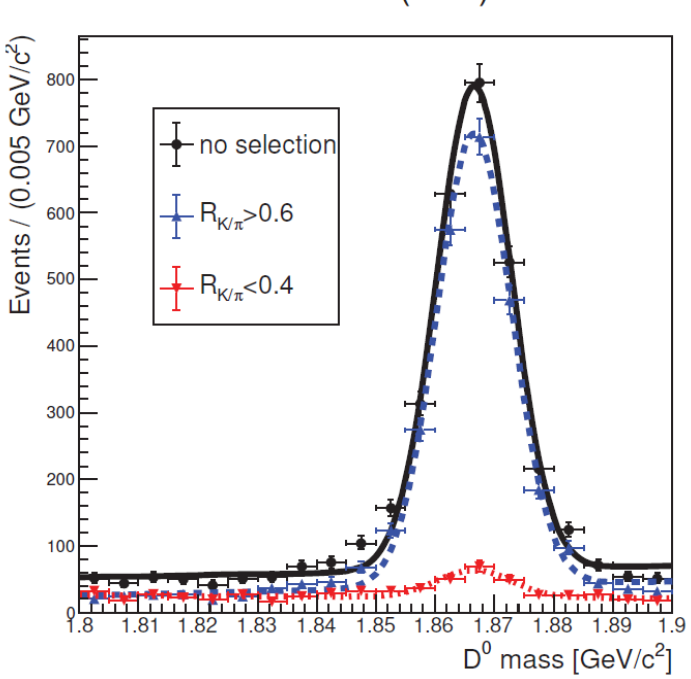

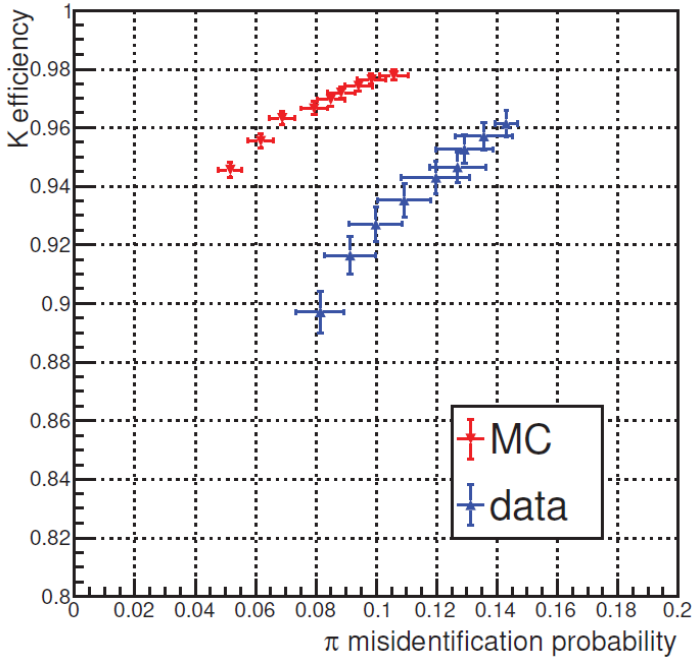

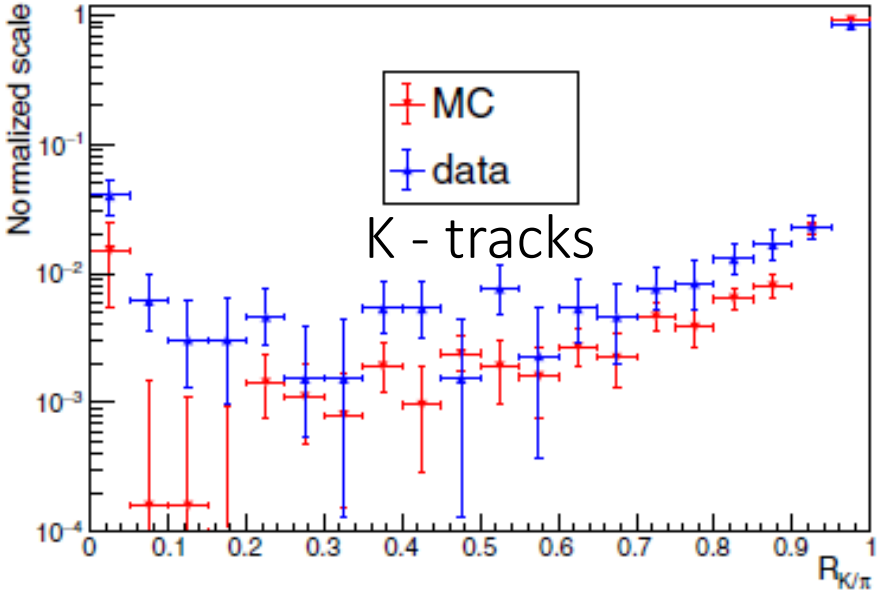

Performance results for 2019 data and MC.

K tracks

Aerogel tile alignment

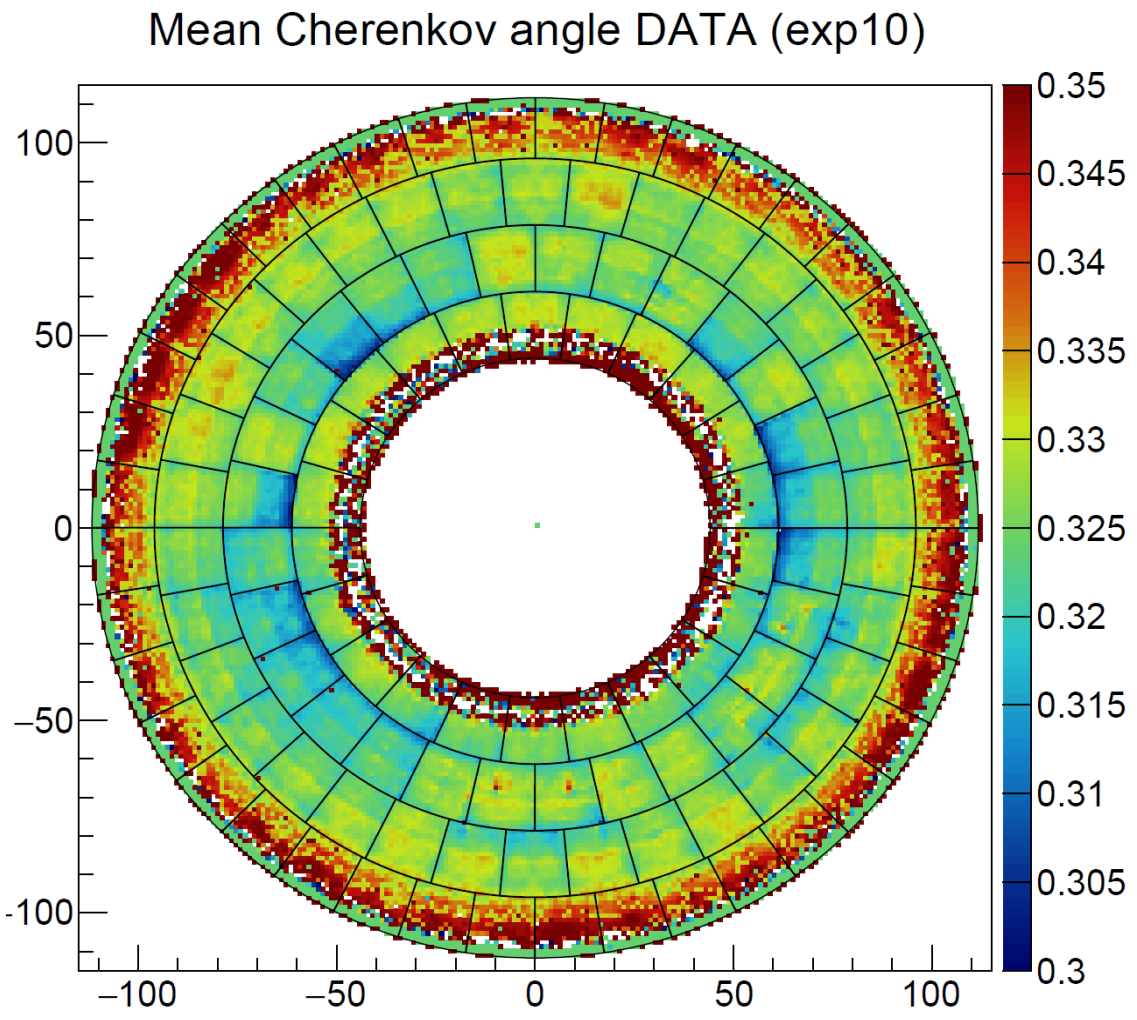

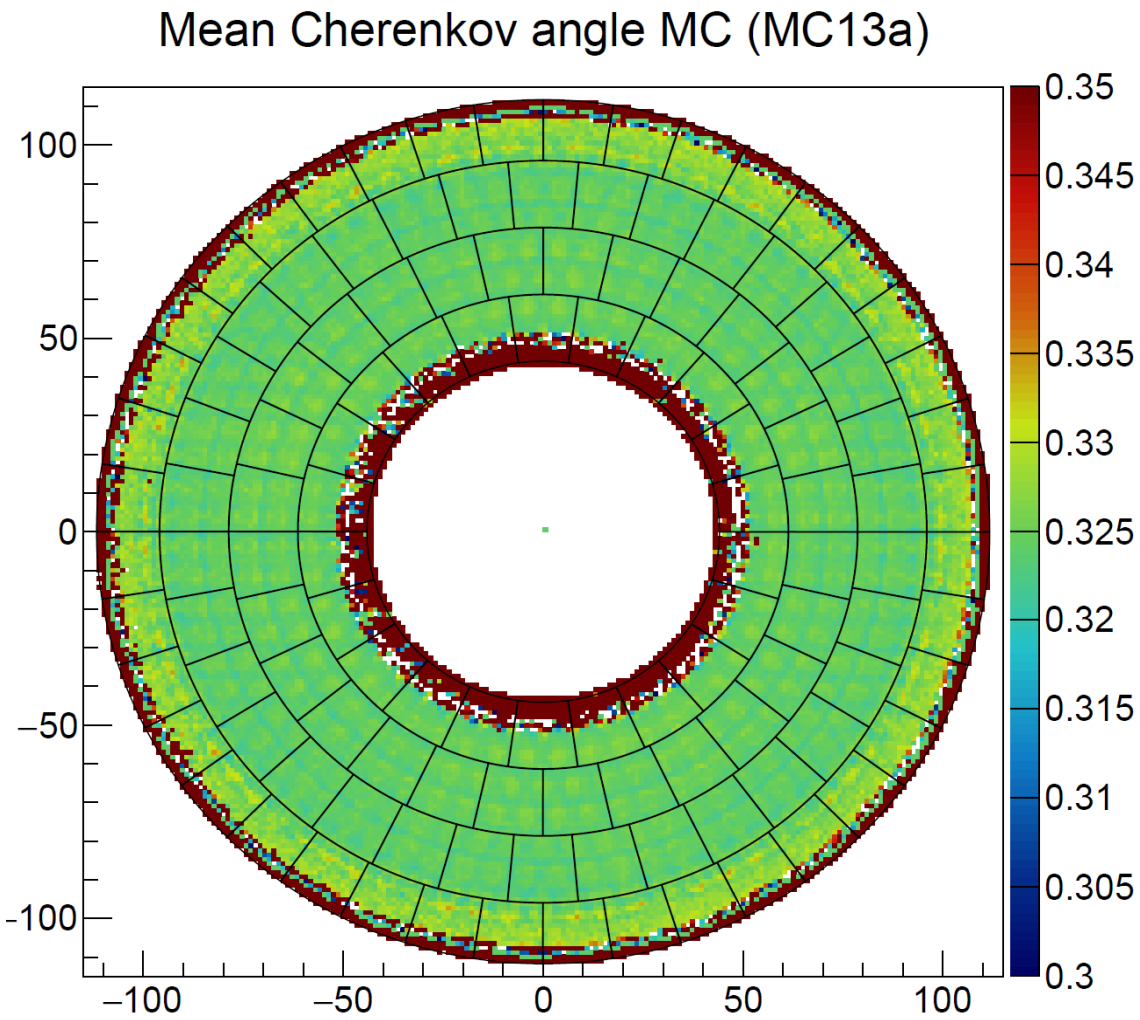

- Aerogel tiles positions and rotations are aligned to get uniform mean cherenkov angle.

Updated PDF functions

Aditional features of updated PDF functions:

- use of track error parameters
- dependance on azimutal angle
- Cherenkov photons generated in HAPD window:
  - by track
  - by delta electrons from aerogel
- HAPD internal reflection inside the window and from APD surface

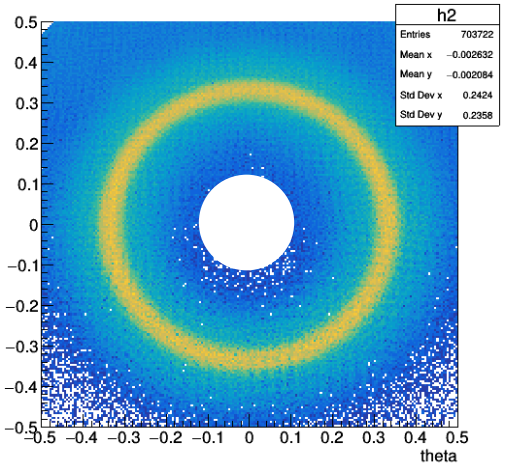

OLD

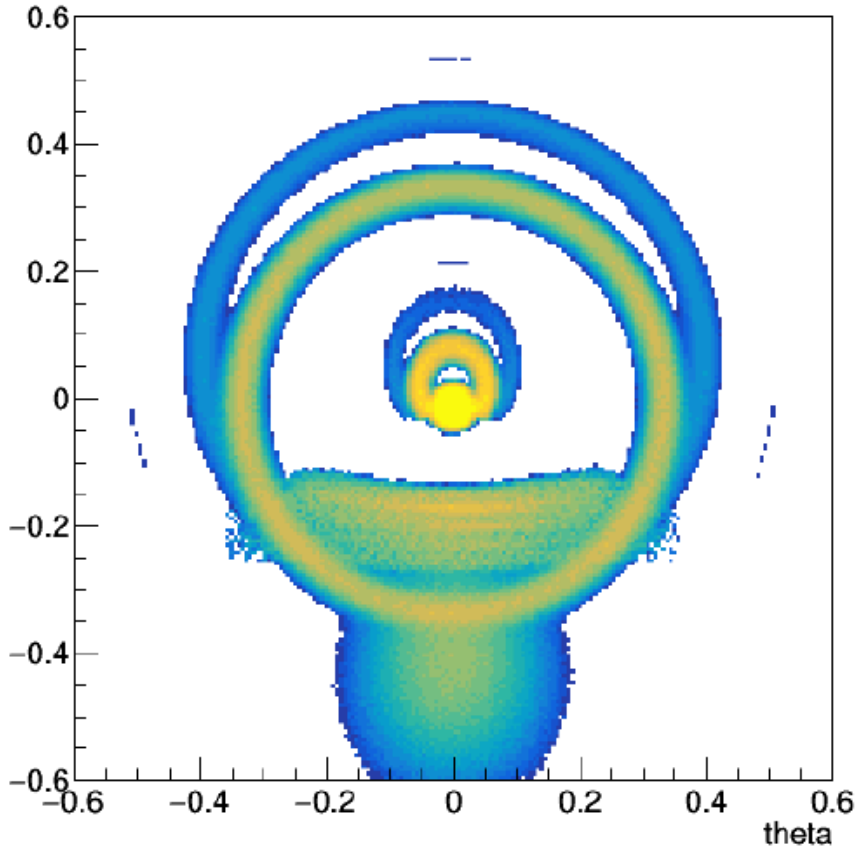

NEW

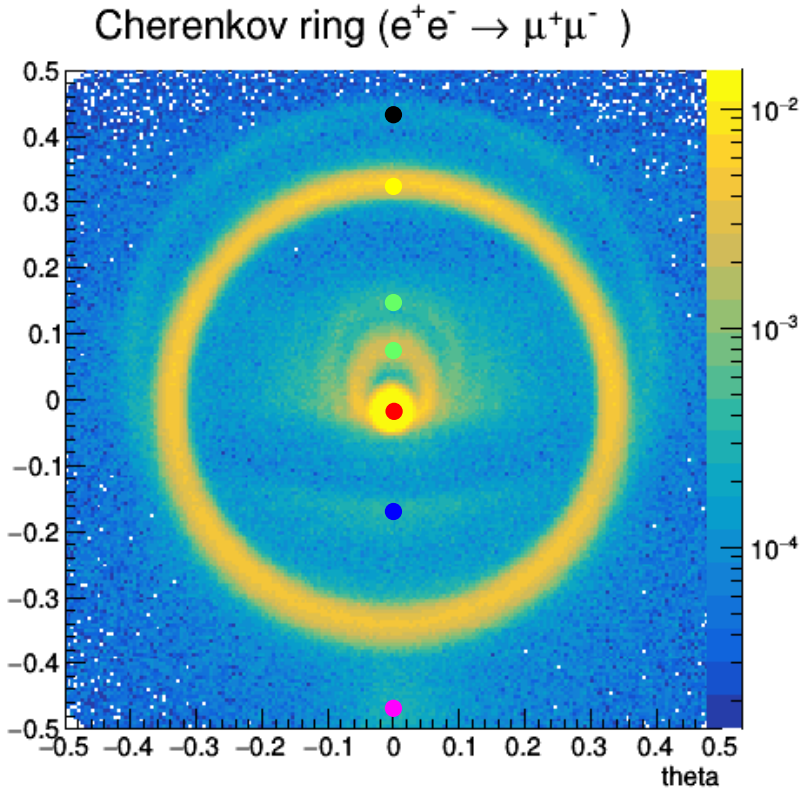

MEASURED

ARICH R&D: Photonis MCP-PMT

Model 85015/A1:

- two MCP steps - chevron configuration
- 8x8 anode pads @6.5 mm pitch, gap ~ 0.5mm
- bialkali photocathode
- gain ~ 0.6 x 10^6 (@2400V)
- 10μm pores → operates up to 1.5 T
- size ~ 59mm
- effective area fraction ~ 80%
- excellent timing < 40ps - single photon
- window thickness 1.5mm

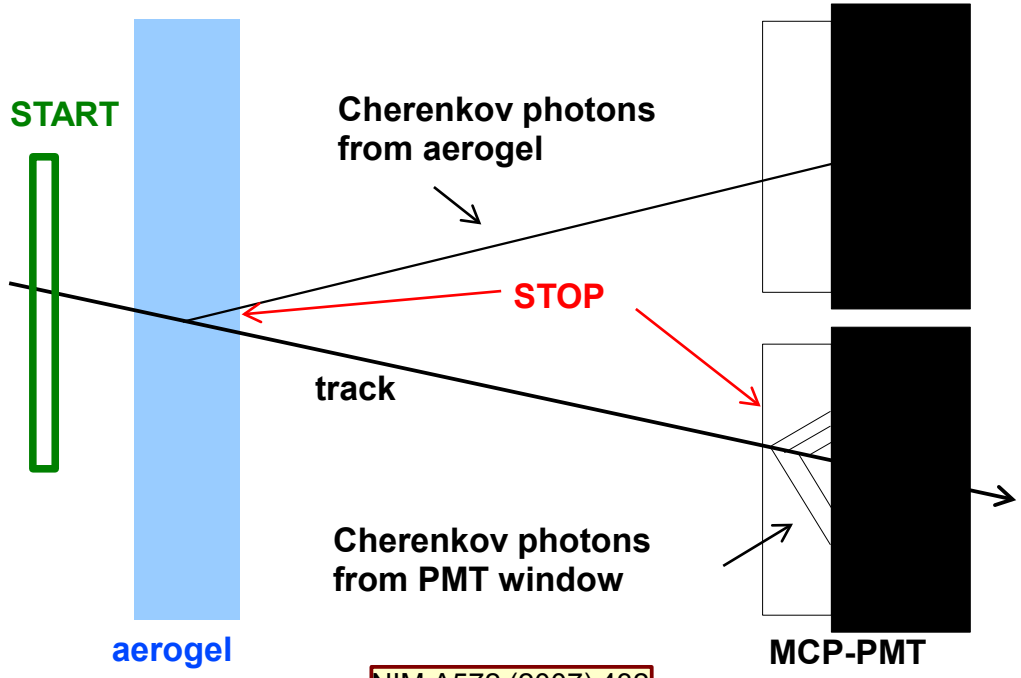

NIM A572 (2007) 432

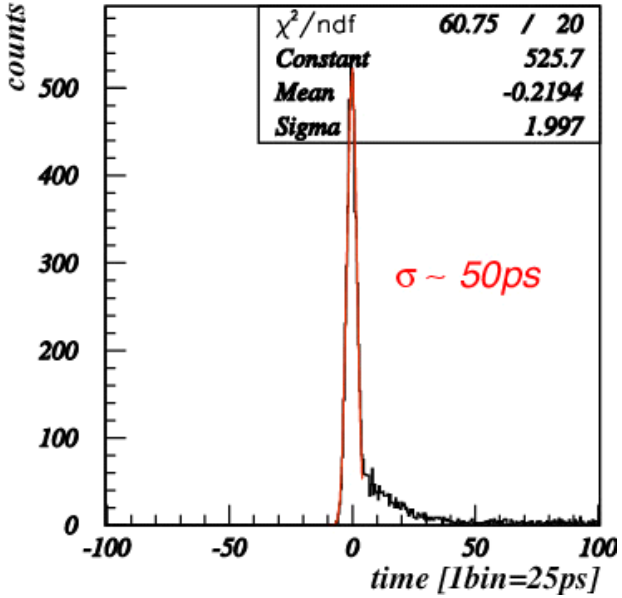

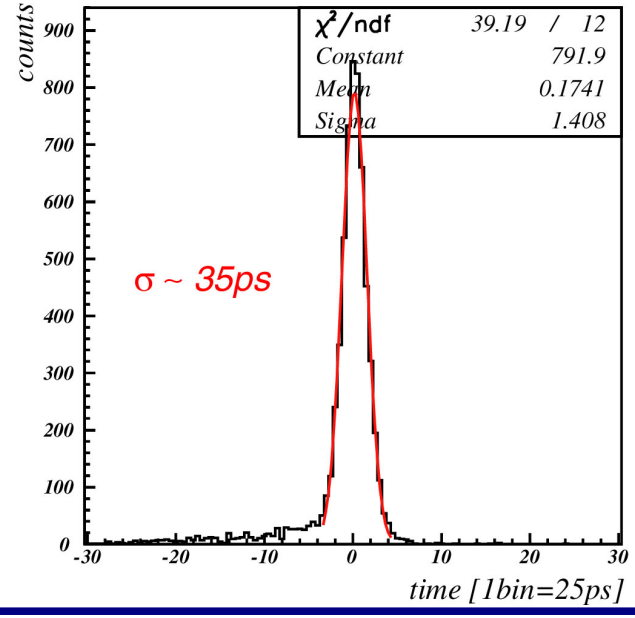

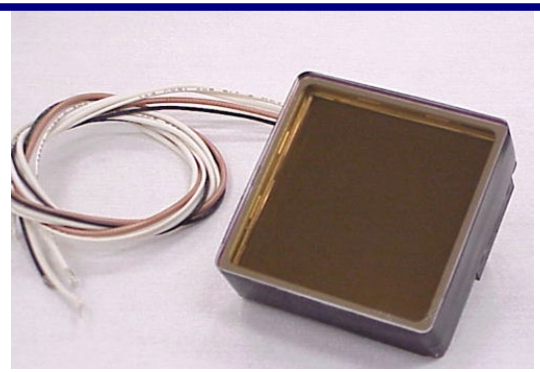

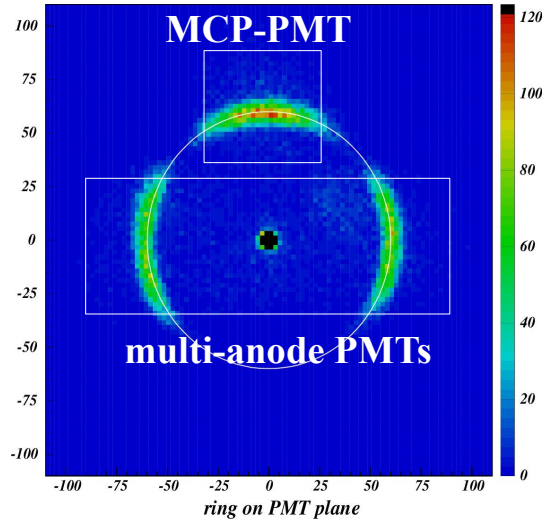

Beam test result of 25μm sample:

- σ_ϑ~13 mrad (single cluster)
- number of clusters per track N ~ 4.5
- σ_ϑ~ 6 mrad (per track)
- → **~ 4 σ π/K separation at 4 GeV/c**

NIM A567 (2006) 124

TOF with ARICH

Using Cherenkov photons emitted in the PMT window (n~1.46) PID can be extended into the lower momentum region:

Kaons and protons can be positively identified below the Cherenkov threshold in aerogel (n~1.05).

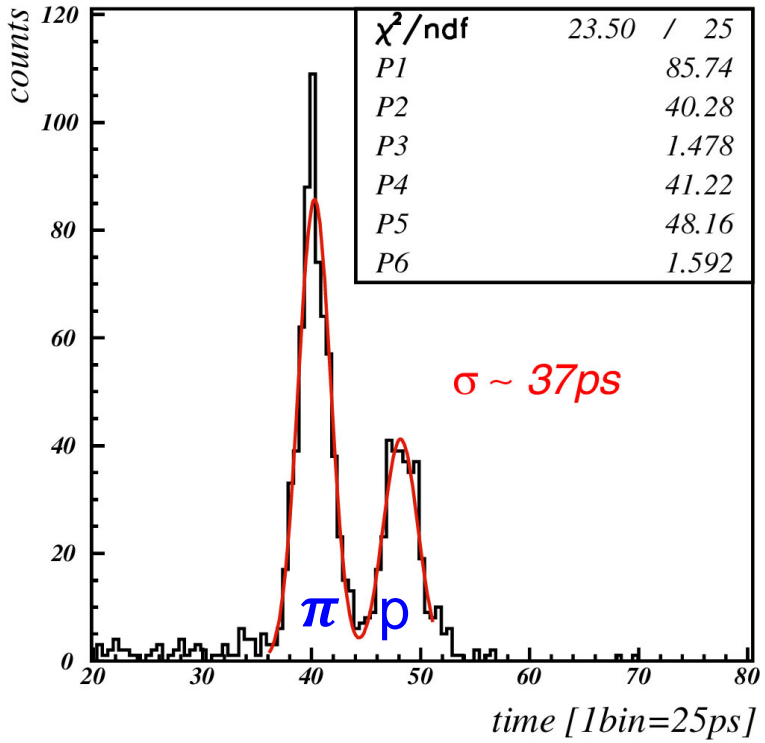

- TOF test with pions and protons at 2 GeV/c

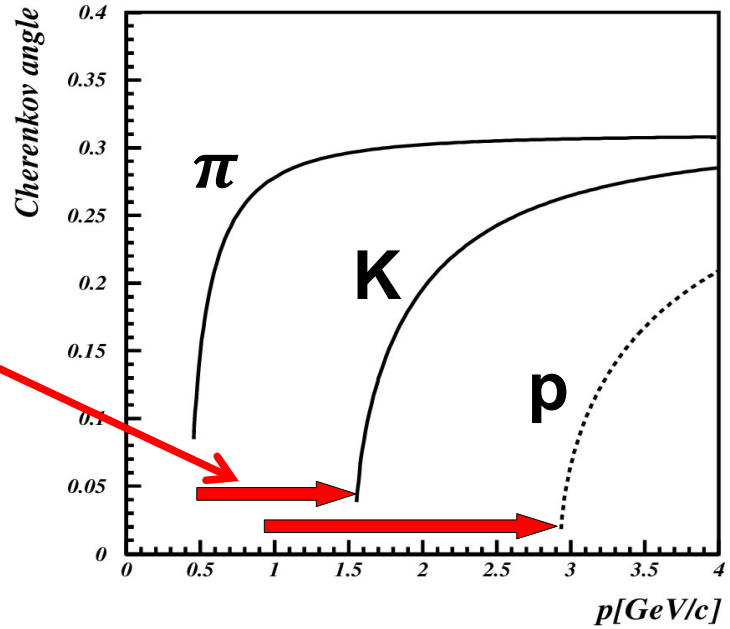

Cherenkov angle in aerogel (n=1.05) for pion, kaon and proton.

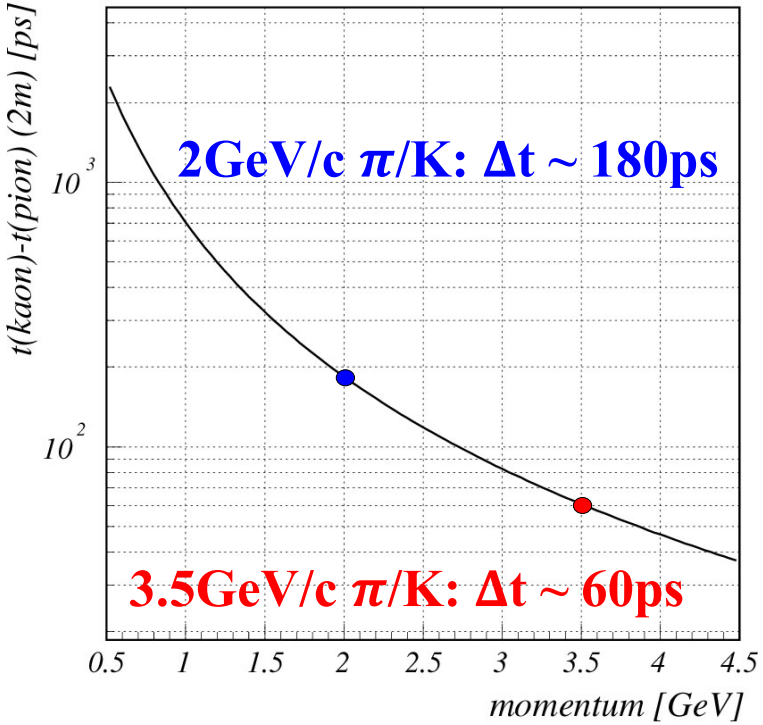

Time-of-flight difference for pions and kaons from IP to forward PID (2m).

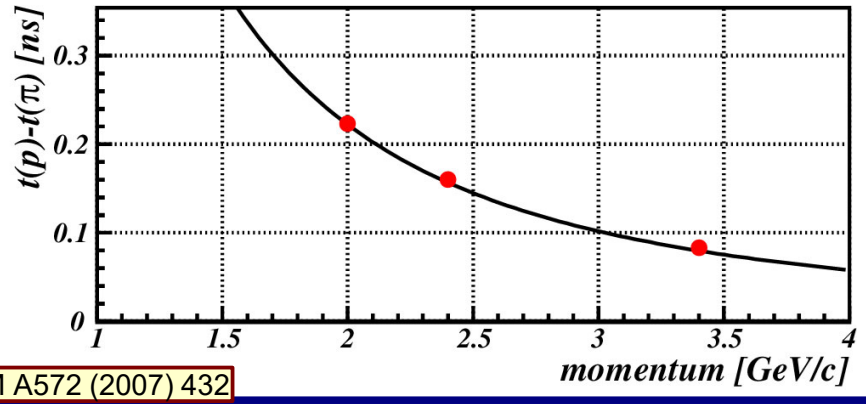

NIM A572 (2007) 432

- distance between start counter and MCP-PMT is 65cm

Single timing channel per module

- electronics for ARICH + TOF could be simplified if a common electrode signal could be used for timing and signals from anode pads for position

- MCP-out signal was tested for common timing

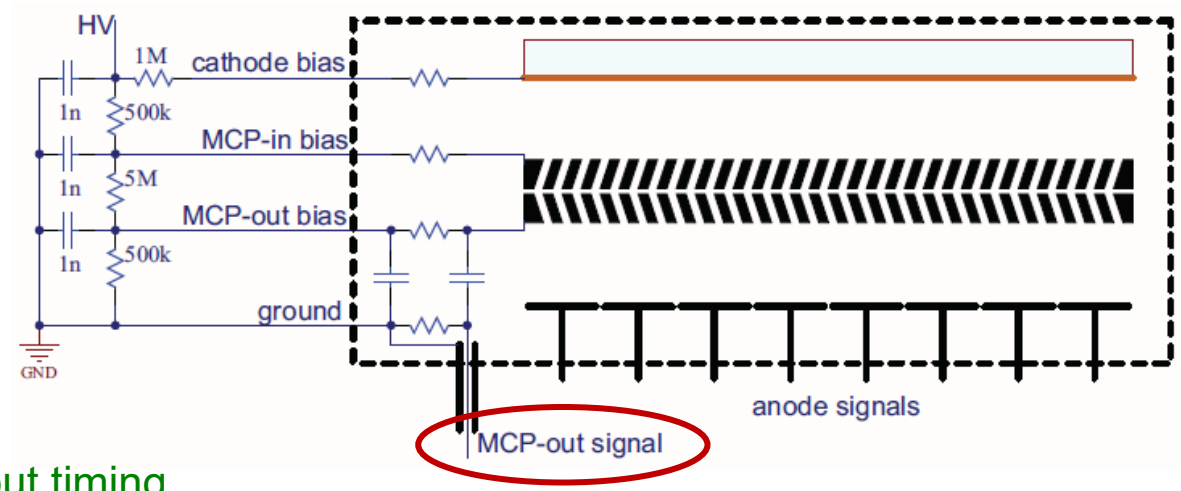

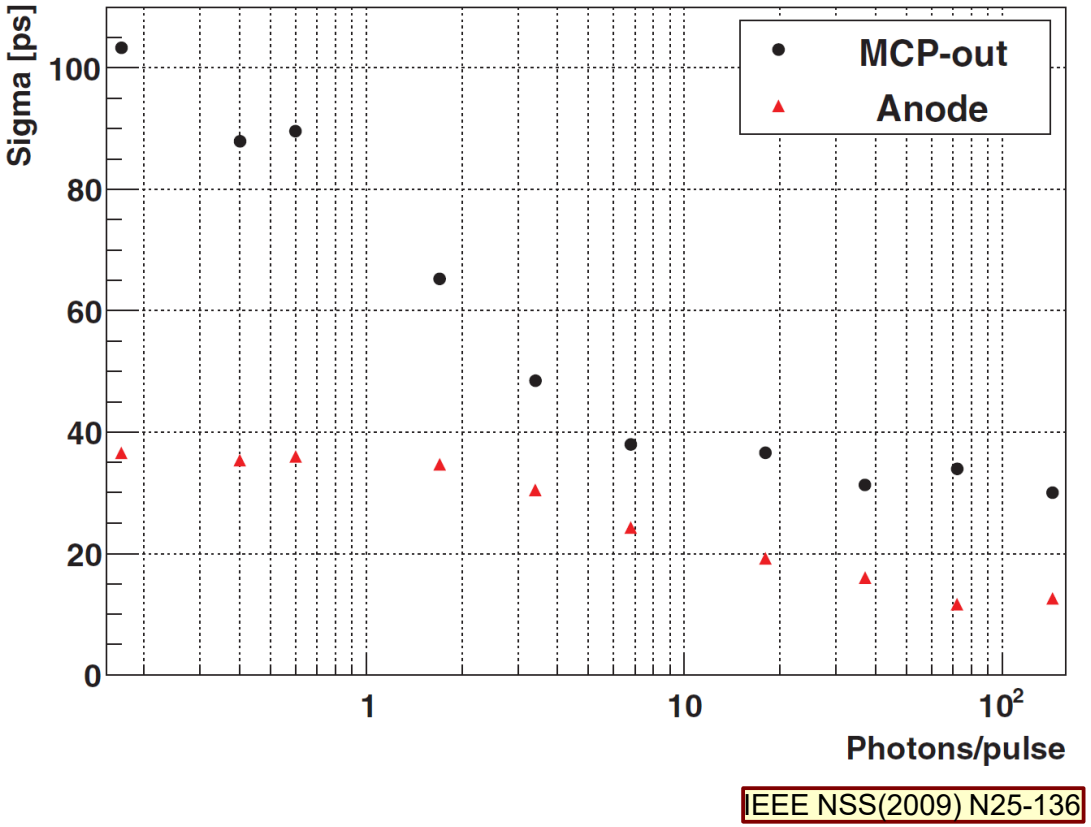

- MCP-out timing resolution vs. average number of photons in the laser pulse

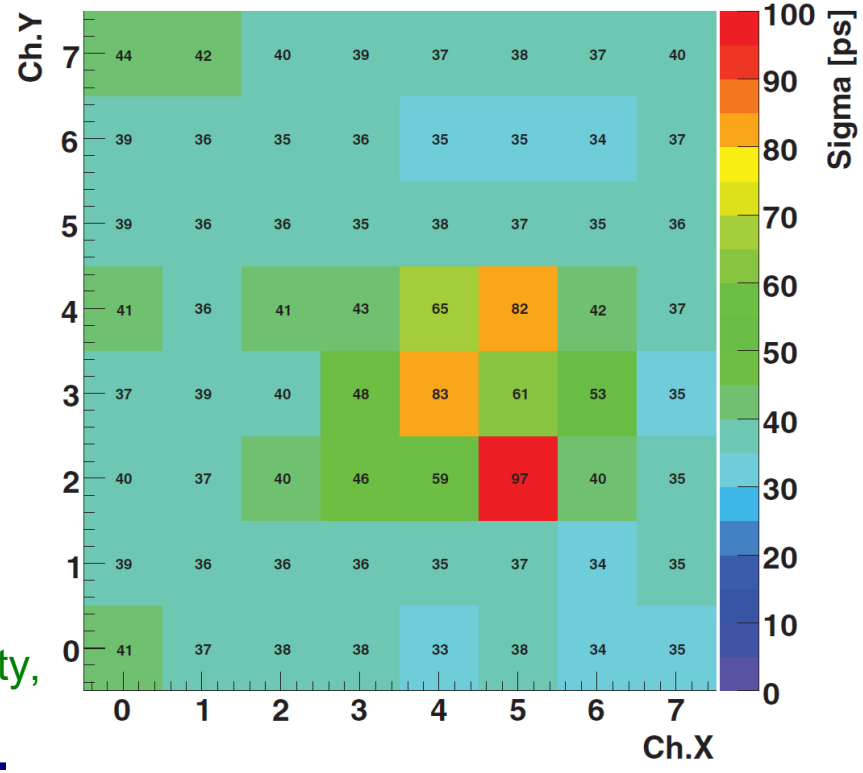

- MCP-out timing resolution uniformity, ≈ 10 photons

SiPM for ARICH: early tests

ARICH photon detector module prototype:

- Hamamatsu 64 channel MPPC module S11834-3388DF, 8×8 array of $3 \times 3\ mm^2$ SiPMs @ $5\ mm$ pitch
- matching array of quartz light concentrators used
- two $20\ mm$ thick aerogel tiles in focusing configuration $(\mathrm{n} = 1.045, 1.055)$
- tested in $5\ GeV$ electron beam at DESY
- estimated 36 hits on full ring

- electronics with < 1 ns resolution
- radiation hardness – DCR increase by neutron irradiation
- cooling

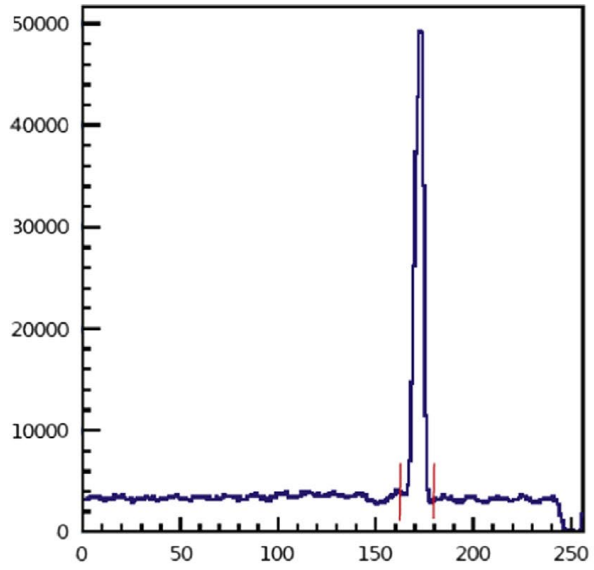

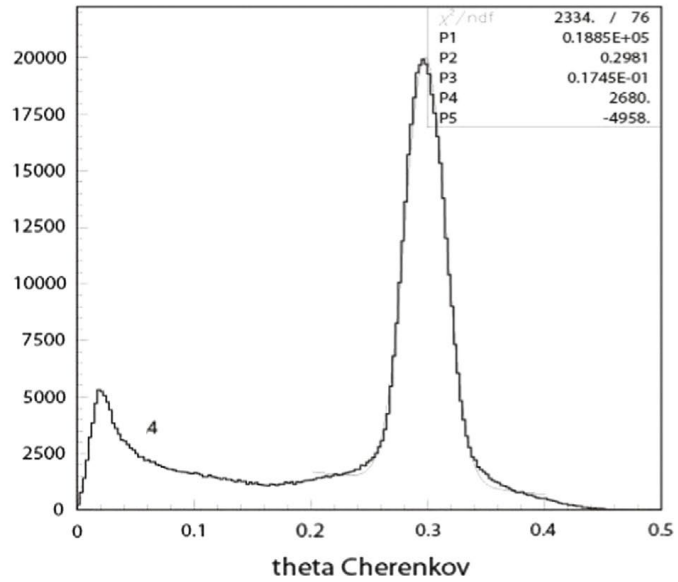

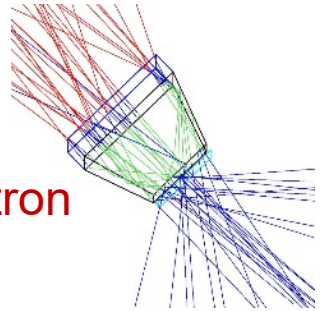

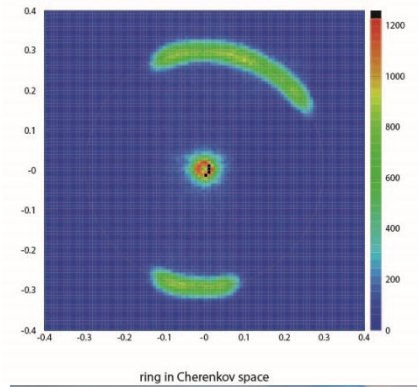

NIM A766(2014)107

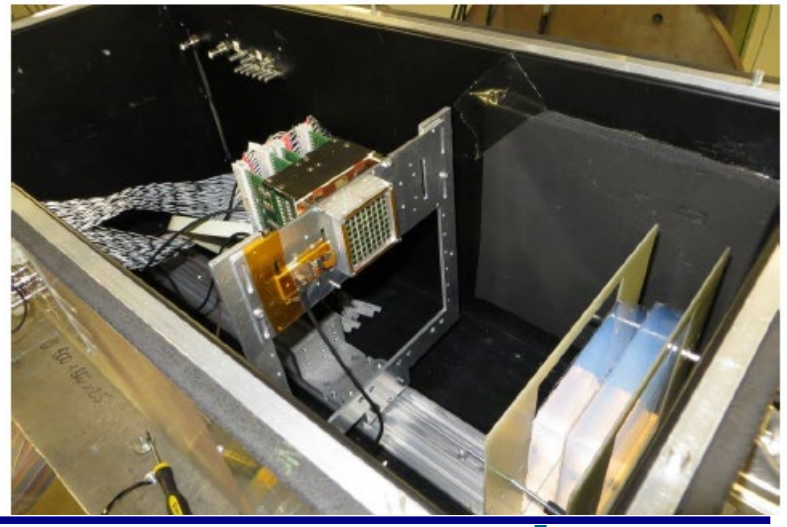

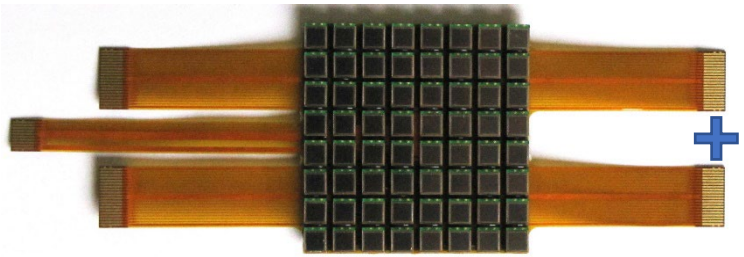

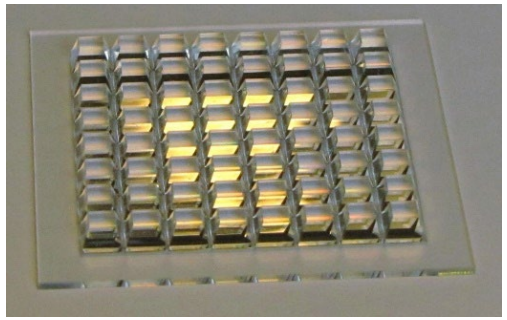

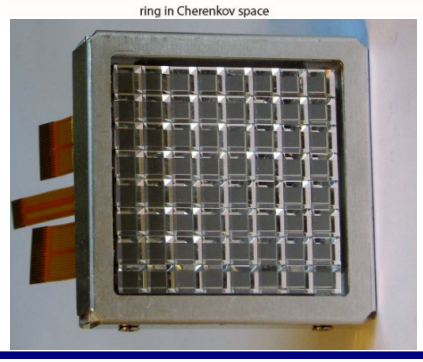

Belle II eksperiment @ SuperKEKB

- Belle II spectrometer sits at the interaction point of SuperKEKB collider - upgraded KEKB
- $7\ \mathrm{GeV}$ electrons and $4\ \mathrm{GeV}$ positrons collide with a centre of mass energy of Υ_{4S} resonance mass.
- Target is to reach integrated luminosity $50\ \mathrm{ab}^{-1}$ by 2031, by 30x higher peak luminosity.
- More challenging for detectors:
  - $30\ \mathrm{kHz}$ trigger rate
  - higher background
  - radiation tolerance.